Breaking the Gridlock of Spatial Correlation in GPS-aided IEEE 802.11p-based Cooperative Positioning

Gia-Minh Hoang, Benoît Denis, Jérôme Härri, *Member, IEEE,* Dirk T.M. Slock, *Fellow, IEEE*

***Abstract*—Spatial correlations found in vehicular mobility are jeopardizing the precision level of Cooperative Positioning (CP) for future Cooperative - Intelligent Transport System (C-ITS) applications. Bayesian filters traditionally assume independence of the measurement noise terms over space between different vehicles and over time at each vehicle, whereas they are actually correlated due to the local continuity of physical propagation phenomena (e.g., shadowing, multipath…) under highly constrained vehicular mobility. In this paper, we break this gridlock by proposing an innovative data fusion framework capable of mitigating these effects to maintain the positioning precision level under severely correlated environments. We first illustrate the dramatic impact of correlated noise affecting both GPS and Vehicle-to-Vehicle (V2V) received power observations. Then we propose a new generic data fusion framework based on Particle Filter (PF) supporting three complementary methods to decorrelate measurement noises in a globally asynchronous context. Comparatively to conventional cooperative positioning, simulations performed in canonical vehicular scenarios (highway, urban canyon, tunnel) show that our proposed approach could provide up to 60% precision improvement in correlated environments, while matching by less than 15–20% deviation an optimal cooperative positioning scheme considered under independent measurements.**

***Index Terms*—Cooperative positioning, Correlated noise, Data fusion, GPS, DSRC, IEEE 802.11p, ITS, VANET.**

I. Introduction

GEO-LOCALIZATION is a critical requirement of future Cooperative - Intelligent Transport Systems (C-ITS) enabling advanced safety and traffic efficiency services. The currently proposed C-ITS Basic Set of Applications (BSA) [1] relies on the availability of the Global Navigation Satellite System (GNSS), which provides a positioning precision on the order of 3–10 meters in favorable conditions [2]. This is obviously far from being sufficient for applications such as for Road Hazard Warning (RHW), Vulnerable Road Users (VRU) safety, Highly Autonomous Driving (HAD) or even platooning. The latter applications would indeed require a sub-meter precision level (typically less than 0.5 m) *in any condition*, which is not yet available with mass market GNSS technologies (incl. Galileo) [1], [3].

Dedicated Short Range Communication (DSRC) (a.k.a. IEEE 802.11p or ITS-G5), a vehicular-specific WiFi extension, has been rapidly developing to enable wireless communications between vehicles (V2V), infrastructure (V2I), and devices belonging to the Internet of Things (V2IoT). Each vehicle periodically broadcasts, through Cooperative Awareness Messages (CAMs) in Europe [4] or Basic Safety Messages (BSMs) in the U.S. [5][1], its GPS-aided estimated position, allowing neighboring vehicles to generate a cooperative situation awareness of their nearby traffic and thus, potential danger. Such cooperative vehicular communications provide a unique opportunity to enhance geo-localization through Cooperative Positioning (CP) [1], [3], [6]–[9]. As illustrated on Fig. 1, instead of considering only Road Side Units (RSUs) as static anchors, CP integrates additional neighboring vehicles as "virtual anchors", using their periodically broadcast CAM primarily to receive and fuse embedded GNSS data (raw or refined), but also optionally, to measure range-dependent radio metrics (e.g., Received Signal Strength Indicator (RSSI)) in an opportunistic way. In comparison with non-cooperative approaches, CP does not require any prior map containing predefined anchor nodes' locations but simply benefits from other vehicles' data and communications.

Despite the significant geo-localization improvements expected with CP (in particular in GPS denied environments), the intrinsic mobile nature of both "virtual anchors" and vehicular wireless channels makes that the indicated GNSS/GPS[2] positions, as well as the received power over V2V links, are still conditionally subject to strong errors and harmful fading conditions respectively. Beyond, CP is also prone to even more specific challenges. First of all, the transmission intervals between consecutive CAMs are constrained by channel load conditions, leading to non-periodic transmission and accordingly, to non synchronous data reception from "virtual anchors". If not appropriately addressed (e.g. [1], [6]), this can lead to severe geo-localization errors. Another challenge is related to restrictions in the application of the core fusion filters when assuming that the GPS/RSSI readings integrated

This work has been performed in the frame of the *HIGHTS* project, which is funded by the European Commission (636537-H2020). EURECOM acknowledges the support of its industrial members, namely, BMW Group, IABG, Monaco Telecom, Orange, SAP, ST Microelectronics, and Symantec.

G.M. Hoang is with the Laboratory of Electronics and Information Technology (LETI), French Commission for Atomic and Alternative Energies (CEA), 38054 Grenoble Cedex 9, France, and also with the Mobile Communications Department at EURECOM, 06904 Sophia Antipolis, France (email: giaminh.hoang@cea.fr).

B. Denis is with CEA-Leti, 38054 Grenoble Cedex 9, France (email: benoit.denis@cea.fr).

J. Härri and D. T.M. Slock are with the Communication Systems Department at EURECOM, 06904 Sophia Antipolis, France (emails: {jerome.haerri,dirk.slock}@eurecom.fr).

[1] Due to equivalent roles played by CAMs and BSMs in our work, we will only refer to CAMs for simplicity, without loss of generality.

[2] Due to equivalent challenges of any GNSS technology in our work, we will interchangeably use GNSS and GPS for simplicity, without loss of generality.

as observations are affected by white error processes whereas in practice, they are strongly correlated over both space and time [1], [10]–[14]. Practically speaking, the spatial correlation of observed measurement processes (and hence, their time correlation under vehicles mobility) results from the conjunction of different factors triggered by constrained vehicular mobility: GPS conditions (good or bad) may not change much over multiple samples and between neighboring vehicles. Similarly, the channel fading conditions (obstructed or not) may not change much between two subsequent transmissions of CAM (e.g. 100 ms) by neighboring vehicles. The direct incorporation of correlated measurements into conventional fusion filters then leads to inconsistent estimates with large fluctuations [15], [16].

In this paper, we thus specifically aim at mitigating the harmful effects of such spatial correlation phenomena with an innovative cooperative positioning approach capable of resynchronizing and decorrelating GPS/RSSI observations under vehicular mobility. The main paper contributions can be summarized as follows: (i) we provide concrete illustrations of the impact of correlated GPS/RSSI data on state-of-the-art CP performance in the vehicular Ad hoc NETwork (VANET) context under steady-state mobility regimes; (ii) in a globally asynchronous V2V context, we describe a new data fusion framework coupling a particle filter (PF) with several decorrelation mechanisms at both signal level (using empirical measurement cross-correlations or forming differential measurements relying on estimated velocities) and/or protocol level (impacting Tx and/or Rx policies); (iii) we adapt typical 2-D GPS noise maps and 4-D V2V RSSI shadowing map from [17] to model correlated observation noises for realistic performance evaluation in our VANET context; (iv) based on these models, we evaluate the proposed approaches in three representative scenarios (i.e., urban canyon, tunnel, and highway scenarios) based on Monte Carlo simulations.

The paper is organized as follows. In Section II, we describe the general background on GPS-aided IEEE 802.11p-based CP. We then state the generic CP problem and stakes, before introducing more specifically the correlated observation models and related issues in Section III. Next, in Section IV, methods alleviating correlation effects are suggested and integrated in a modified particle filter dedicated to fusion-based CP in GPS-aided VANETs. Simulation results illustrate the achievable performance gains in comparison with more conventional CP approaches in Section V. Finally, Section VI concludes the paper and provides an outlook on future works.

II. Background on GPS-aided IEEE 802.11p-based Cooperative Positioning

A. Cooperative Communications in VANETs

In the field of vehicular communications, cooperation relates to vehicles regularly exchanging their sampled status (e.g., timestamp, GNSS position, motion state…) and attributes (e.g., specifications of the vehicle) via DSRC to create and maintain cooperative awareness [3]–[5] (see Fig.1). DSRC[3] is

[3]DSRC shall not be confused with CEN DSRC in Europe, which refers to a dedicated communication solution for toll roads.

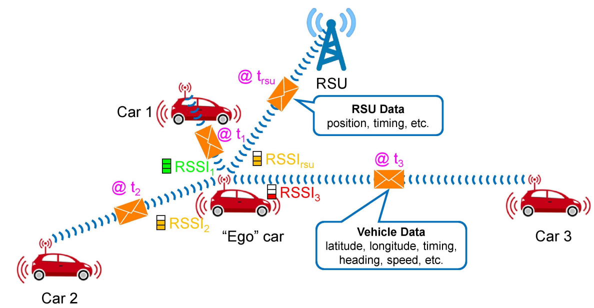

Fig. 1. Cooperative cars periodically exchange CAM messages to maintain awareness of each other and to support distributed CP. Both the transmission time $@t_i$ and the received power level $RSSI_i$ depend on the transmission car i (and thus, on the V2V link).

a vehicular-specific extension of the WiFi 802.11a capable of operating on a 10 MHz dedicated frequency band at 5.9 GHz, outside the context of a Basic Service Set (BSS). These status and attributes are encapsulated in CAMs and scheduled for transmissions by a congestion control mechanism according to vehicles dynamics and channel conditions. As illustrated in Fig.1, an "ego" car may therefore benefit from its neighbors, which have sent their CAMs at different times instants ($@t_i$). To be beneficial for multilateration purposes (i.e. measuring the relative distances between the different neighbors), these messages would need to be roughly received at similar times, and the range-dependent information uniquely extracted from the CAM RSSI readings at the "ego" vehicle.

Congestion control mechanisms are intended to provide dependable vehicular communications for safety-critical applications. Different mechanisms are defined in standards [4], but adjusting the transmit power of CAM and the inter-transmit time between two successive CAMs are the two leading mechanisms. Both approaches are expected to lead to major drawbacks to CP if not properly addressed by fusion engines. First, when using RSSI readings as range-dependent measurements, it is assumed that all "virtual anchors" are transmitting at the same transmit power. Uncoordinated transmit power adjustments lead to inconsistent range estimations from RSSI readings. Second, by using CAM for RSSI readings and GNSS data, it is assumed that CAM are received at the "ego" vehicle in a roughly synchronous way (similar $@t$). However, uncoordinated CAM inter-transmit times lead to a time lag between the different anchor measures and to asynchronous inputs to fusion engines. Jointly or separately, these congestion control mechanisms lead to increasing rather than reducing geo-localization errors.

In this paper, we address these challenges by assuming a constant transmit power for all vehicles and by proposing a fusion engine that enables CAM data re-synchronization.

B. Cooperative Positioning in VANETs

In the field of wireless localization, cooperation is generally intended in an even more specific sense. Whereas so-called non-cooperative schemes aim at geo-localizing mobile nodes uniquely with respect to a set of fixed anchors at known locations, CP solutions make use of neighboring nodes (moving or static) as additional "virtual anchors" [18], typically through distributed message-passing approaches [19]. Such CP schemes have been successfully applied to static Wireless Sensor Networks (WSNs) or even Mobile Ad Hoc Networks (MANET). However, due to the particular mobility patterns and route constraints, frequent network topology fragmentation, short link life time (e.g., 1 second for vehicles traveling in opposite directions), applying CP to VANETs still remains challenging.

Considering non-cooperative positioning in the vehicular context, static elements of the road infrastructure, such as Road Side Units (RSUs) or LTE eNBs, are considered as anchors, and vehicles independently estimate their locations through classical multilateration (i.e., measuring the relative distances between the anchors), range-free cell connectivity information (possibly combined with dead-reckoning [20]), or even fingerprinting (e.g., possibly assisted by particle filtering [21]). However these solutions strongly depend on the density, the availability and the relative geometry of the road infrastructure. For instance, as illustrated on Fig. 1, one single V2I link with respect to a RSU would be insufficient to get the "ego" vehicle positioned through standard multilateration with no ambiguity.

On the contrary, CP allows to complement these static anchors with neighboring vehicles to integrate additional position awareness and opportunistic V2V radio link measurements [3], [7], [16], [19], as shown on Fig. 1. For instance, the authors in [9] propose a distributed tracking algorithm relying on a standard Kalman Filter (KF), which fuses GPS position estimates with nearby anchor nodes' positions and V2V range measurements (assumed to be perfect) after detecting harsh GPS conditions. As another example, the cooperative solution in [8] is based on a dissimilarity matrix composed of V2V RSSI measurements. The latter are injected as observations into an Extended KF (EKF), while using GPS estimates for initialization purposes only. In [7], the V2V measurements matrix and the GPS position are jointly incorporated as observations in the filter. In [6], GPS positions and V2V RSSI measurements are also combined within a global EKF framework, while compensating for asynchronous input data.

Most of the above cooperative schemes still rely on too simplistic or optimistic assumptions in terms of propagation (e.g., regarding V2V RSSI shadowing dispersion and 2D correlation, GPS error correlation…), network connectivity (e.g., transmission range, instantaneous number of available neighbors…) and/or protocol constraints (e.g., asynchronous transmissions, power and rate control…). Moreover the achieved level of accuracy (equivalent to that of nominal GPS in favorable operating conditions) is still largely insufficient for the foreseen safety-oriented applications. In a globally asynchronous context, the approach described in this paper thus aims at fusing local GPS information (whenever available) with both measured RSSIs with respect to neighboring vehicles (i.e., out of their received CAMs) and GPS position estimates provided by these neighbors (i.e, resulting from their own fusion processes), while considering jointly realistic propagation, mobility and protocol constraints. The combination of V2V and GPS information in distributed contexts raises unprecedented challenges that require in-depth understanding and careful assessment, as presented in the next subsection.

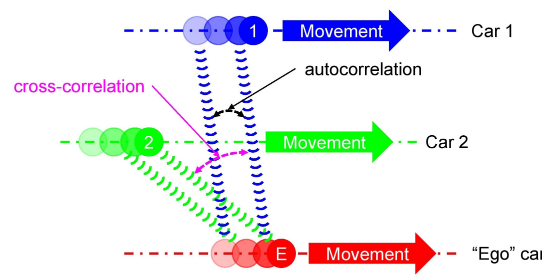

Fig. 2. Possible shadowing autocorrelations/cross-correlations on/between V2V link(s) having dual mobility in VANETs.

C. Correlated Position Errors and Fading

In GPS-aided VANETs, GPS positions and V2V power measurements (or RSSI readings) used for positioning are measured over noisy propagation channels. Generally speaking, these noises are both time-variant and space-variant under typical vehicular mobility (on highways or in urban areas).

On the one hand, time-variant noise can be filtered out by averaging the signal in time or frequency domains (e.g. small-scale fading in RSSI measurements) [10] or using correction models at receivers and information broadcast by transmitters (GPS satellite clock errors or atmospheric errors) [11].

On the other hand, location-dependent measurements are more challenging as they are significantly impacted by the physical arrangement of surrounding objects in the environment (e.g., buildings, trees, hills…) [22]. More specifically, the spatial correlation of observed measurement processes and thus, their time correlation under car mobility, partly results from the local continuity of electromagnetic interactions in the environment. For GPS position estimates and V2V range-dependent power respectively, multipath (often dominating the error budgets) [11] and shadowing (i.e., large-scale or slow fading) [10] are major sources of spatial correlation, especially under constrained mobility patterns and/or constrained acquisition time intervals.

As an example, a GPS receiver can experience very large 2-D positioning errors in a narrow street, due to its limited visibility to satellites (i.e., few available satellites causing poor geometric dilution of precision, biased pseudo-range measurements due to GPS signal diffraction on building edges...). Intuitively, while moving along the street, these GPS errors will remain of the same order of magnitude for a few tens or even hundreds of meters and as such, will be spatially correlated. The extent of such GPS spatial correlation depends on the environment. In urban canyons, both the number of available satellites and the multipath propagation conditions shall remain unchanged over a distance equivalent to the width of a typical building. In more open-sky environments (e.g., on highways), these conditions remain unchanged over much larger distances. Generally speaking and regardless of the environment, this spatial correlation is always present in VANETs and definitely impact the use of GPS data.

Spatial correlation also exists for V2V propagation channels (i.e., in terms of slow fading characteristics). They may be intuitively explained by both the relative network topology and the local link obstruction conditions (e.g., generated by the transmitting/receiving cars' bodies themselves, by non-

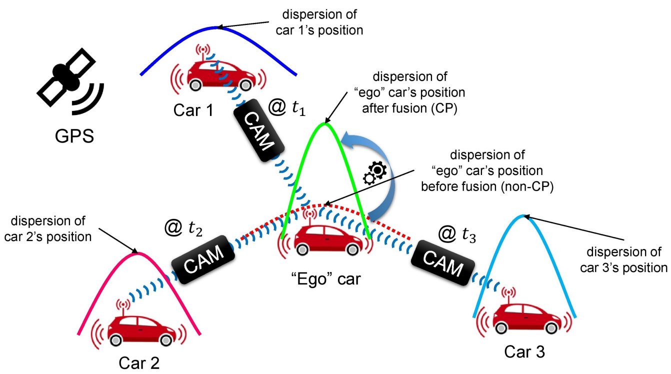

Fig. 3. "Ego" car receiving asynchronous CAMs from 1-Hop "virtual anchors" to perform distributed CP. The dispersion of CP location estimates (i.e. through GPS+DSRC) is expected to be lower than that of non-CP estimates (i.e., standalone GPS).

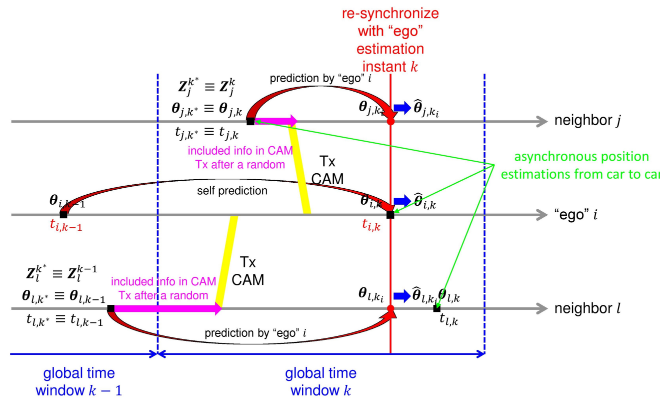

Fig. 4. Example of the space-time schematic managed by the "ego" i whose neighbors are vehicle j and l. Due to asynchronous estimates, the "ego" i needs to perform prediction of received information at its time of interest $t_{i,k}$.

cooperative trucks, by pieces of urban furniture...), which evolve slower under constrained mobility patterns (e.g., platooning on highways, queuing vehicles during rush hours in urban canyons...) than the time intervals between successive transmissions (i.e., 1–10 Hz [4], [5]). Regardless of the environment, spatial correlations in V2V propagation channels thus impact all the vehicles involved in range-dependent information estimation (i.e., based on RSSI readings). An illustration is provided on Fig. 2. Considering the V2V link between the "ego" car and "car 1", successive RSSI readings are autocorrelated if the inter-transmit times between packets are larger than the rate change of their mobility patterns and fading conditions. Similarly, considering the two V2V links between "ego" car and "car 1" and "car 2", successive RSSI readings are cross-correlated if the inter-transmit times between packets are larger than the rate change between the mobility patterns of "car 1" and "car 2". Depicted on Fig. 2 for V2V measurements (RSSI readings), cross-correlations and autocorrelation also impact the use of GPS information at the "ego" car. Successive CAM transmissions of the GPS information from "car 1" and from "car 2" will indeed integrate also GPS spatial correlation (as previously described) if their inter-transmit time is higher than the time to move over the GPS decorrelation distance.

Summarizing, widely observed and reported in GNSS and V2V fading literature [1], [10]–[14], [23], spatial correlations are yet hardly addressed in previous works dealing with distributed and/or cooperative positioning in the vehicular context. It is however essential to consider a realistic observation model with correlated noises (on both GPS and V2V RSSI observation ingredients) in order to avoid producing biased and/or unreliable results while assessing CP performance.

III. Problem Formulation

A. Generic Cooperative Positioning

We consider here a set of cooperative GPS-equipped vehicles exchanging CAMs over a typical DSRC technology. The goal of an "ego" vehicle is to infer its position (as part of its so-called "state" in the following) based on its own estimated GPS position, on V2V received signal strengths with respect to 1-hop neighbors (measured out of incoming CAMs), and on imperfect state information from these neighbors, viewed as "virtual anchors" (i.e., estimated locations and their related uncertainties, encapsulated in the CAMs). Fig. 3 illustrates this CP concept. We do not consider V2I communications here to assist positioning, since we provide a generic problem formulation for all GPS-aided cooperative objects. The use of RSUs is considered as a special but simpler case of the generic problem formulation.

In order to perform CP in pure VANET contexts, the following challenges must be overcome. First, distributed data processing (local position estimation, CAM trigger...) induces event-driven CAM transmissions and accordingly, RSSI measurements too. Hence on the receiver side, the aggregation of asynchronous data (see Fig. 3) makes the whole information misaligned or outdated and thus useless to CP, unless a careful prediction scheme is employed. Second, as already pointed out, as the efficiency of Bayesian filters relies mostly on the assumption of white measurement, spatial correlation effects causing both spatial and temporal correlated GPS positions and RSSI readings yield inconsistent and inaccurate fusion results [1], [12].

B. Filtering Model including Correlated Observations

The mobility model is at the core of any tracking problem, from which many different model-based filtering techniques can be applied. It is generally usual to consider models that are linear and non-linear for state and observation dynamics respectively [24]:

$$\boldsymbol{\theta}_{i,k+1} = \mathbf{F}_i\boldsymbol{\theta}_{i,k} + \mathbf{f}_{i,k} + \mathbf{G}_i\mathbf{w}_{i,k}, \tag{1a}$$

$$\mathbf{z}_{i,k} = \mathbf{h}(\boldsymbol{\theta}_{i,k}) + \mathbf{n}_{i,k}, \tag{1b}$$

where $\boldsymbol{\theta}_{i,k}$ is the state vector of vehicle i collecting the components of interest for the system (e.g., position, velocity, heading,...) at its local discrete time k[4], $\mathbf{F}_i$ the state transition matrix, $\mathbf{f}_i$ the control inputs (e.g., throttle settings, braking forces), $\mathbf{G}_i$ the matrix that applies the effects of each noise component in the process noise vector $\mathbf{w}_{i,k}$, $\mathbf{h}(\boldsymbol{\theta}_{i,k})$ the transformation matrix that maps the state vector

[4]Due to asynchronously sampled time instants, the index k is different from one vehicle to others. For notation brevity, the subscript indicating the "ego" vehicle is deliberately omitted hereafter.

parameters $\boldsymbol{\theta}_{i,k}$ into the measurement/observation $\mathbf{z}_{i,k}$, which is corrupted by a measurement noise term $\mathbf{n}_{i,k}$.

In the vehicular context, a stochastic mobility model such as the Gauss-Markov prediction model, where the predicted 2-D velocity (at a discrete instance) is determined based on its previous sample and a Gaussian independent and identically distributed (i.i.d) process $\mathbf{w}_{i,k}$, may be applied into (1a) [25]. However, the measurement noise $\mathbf{n}_{i,k}$ is commonly correlated and so is the measurement $\mathbf{z}_{i,k}$, which will be analyzed and modeled hereafter.

Generally speaking, the GPS positions of different vehicles are collected asynchronously leading to asynchronous enhanced position estimates (i.e., after filtering/fusion), as shown in Fig. 4. For ease of notations, we consider a global timeline divided into time windows indexed by k so that all the events of position estimates occurring within this time slot granularity share the same index k (See Fig. 4). Throughout this paper, we will use the notations in Table I, some of them being also illustrated in Fig. 4.

Given all the available measurements $\mathbf{Z}_i^k$, the goal of each vehicle is to track its own state (i.e., $\boldsymbol{\Theta}_i^k$), as well as to build and update a local dynamic map (LDM) of its immediate neighbors' locations (i.e., $\{\boldsymbol{\Theta}_j^{k_i}\}$, $j \in \bigcup_k \mathcal{N}_{i,k-1:k}$).

1) GPS Absolute Position: The 2-D position $\mathbf{x}_{i,k}$ is first determined by a GPS receiver and the corresponding measurement $\mathbf{z}_{i,k}^{\text{GPS}} = (z_{i,k}^x, z_{i,k}^y)^\dagger$ is contaminated by additive noise $\mathbf{n}_{i,k}^{\text{GPS}} = (n_{i,k}^x, n_{i,k}^y)^\dagger$, as follows:

$$z_{i,k}^x = x_{i,k} + n_{i,k}^x, \quad z_{i,k}^y = y_{i,k} + n_{i,k}^y. \tag{2}$$

The latter errors affecting 2-D coordinates, $n_{i,k}^x$ and $n_{i,k}^y$, are commonly supposed to be i.i.d centered Gaussian like in [6], [8], [9], for the sake of simplicity. However, as already mentioned, this i.i.d assumption is too optimistic due to the spatial correlation between observations successively collected by a single moving GPS receiver (autocorrelation) and/or between simultaneous observations at nearby receivers (cross-correlation).

Motivated by the common idea of modeling the spatial correlation of shadowing with the exponentially decreasing autocorrelation function (ACF) (Gudmundson's model) [13], we adapt it for GPS residual errors too. This is a fairly reasonable model since its ACF fits well the first order Gauss-Markov process recommended by [26] to model GPS errors. More particularly, this yields:

$$R_{\text{GPS}}^{(\cdot)}(\tau) = \left(\sigma_{\text{GPS}}^{(\cdot)}\right)^2 r_{\text{GPS}}^{(\cdot)}(\tau) = \left(\sigma_{\text{GPS}}^{(\cdot)}\right)^2 \exp\left(-\frac{v\,|\tau|\log 2}{d_{\text{cor}}^{(\cdot)}}\right), \tag{3}$$

where $(\cdot)$ can be either x- or y-coordinate, $\sigma_{\text{GPS}}^{(\cdot)}$ the standard deviation of residual noise in one direction, v the mobile speed, τ the time lag between measurements, and finally $d_{\text{cor}}^{(\cdot)}$ the equivalent correlation distance at which the corresponding normalized ACF is equal to 50%. These correlation distances are of critical importance and can be determined by a prior calibration procedure [10].

To model spatially correlated GPS error components $n^{(\cdot)}(\mathbf{x})$, with $\mathbf{x} = (x, y)^\dagger$ indicating 2-D GPS receiver's position, whose ACF has the exponential decay as in (3), the 2-D correlated GPS error map $\hat{n}^{(\cdot)}(\mathbf{x})$ can be approximated by generating a finite sum of sinusoids (SOS) (e.g., 100) whose periodicity is dependent on the GPS receiver's x- and y-coordinates, as presented in [27]. It is worth noticing that these two spatially correlated GPS errors affecting x- and y-coordinates are generated independently in the present paper for simplicity. This is however compliant with the remark that strong spatial correlation effects usually occur along one single dimension in typical vehicular scenarios (e.g., along a street in urban canyons).

2) V2V Received Power: The RSSI measurements performed out of received CAMs can be modeled as follows:

$$z_i^{j\rightarrow} = P(d_0) - 10 n_p \log_{10}\left(\frac{\|\mathbf{x}_i - \mathbf{x}_j\|}{d_0}\right) + s_i^{j\rightarrow}, \tag{4}$$

where $P(d_0)$ [dBm] is the average received power at a reference distance $d_0 = 1$ m, n_p the path loss exponent, $\|\cdot\|$ the Euclidean distance, and finally $s_i^{j\rightarrow}$, a random shadowing term that is centered Gaussian with standard deviation σ_{Sh}, and usually correlated in space [10], [12]. Again, while using RSSI measurements in the wireless localization context, it is common to remove small-scale fading effects by averaging in either time or frequency domain first [28].

Note that, as a preliminary investigation step, we also focus herein on Line of Sight (LoS) situations. This choice is first motivated by the fact that we are mostly interested in evaluating canonical scenarios under regular steady-state mobility over straight portions of tracks, where correlation effects are more frankly observable and likely more penalizing (See Sec. V). We thus exclude obstructions caused by buildings [29], [30], which occur typically in urban intersection scenarios and are strongly dependent on the buildings kind, size and number. We also discard deliberately mobile Non Line of Sight (NLoS) situations caused by moving cars or trucks (e.g., [31], [32]) since CP is selective and deliberately restricted to the closet ring of neighboring vehicles like in [6], [33], hence limiting drastically the probability of incorporating mobile NLoS observations in the fusion filter.

The correlated V2V RSSI shadowing properties are again modeled by an exponential ACF [13]:

$$R_{\text{Sh}}(\tau) = \sigma_{\text{Sh}}^2 r_{\text{Sh}}(\tau) = \sigma_{\text{Sh}}^2 \exp\left(-\frac{v\,|\tau|\log 2}{d_{\text{cor}}^{\text{Sh}}}\right), \tag{5}$$

where, similarly to (3), v indicates the speed of the vehicle, τ the time lag, and $d_{\text{cor}}^{\text{Sh}}$ the correlation distance at which the shadowing effect is half of its maximum value.
Gudmundson's model was originally proposed to predict shadowing correlations in cellular networks, that is, for radio links between base stations and mobile stations [13]. Accordingly, in the vehicular context, it could be applied as it is uniquely for links with common end points (e.g., V2I links) but not for links involving two mobile extremities (i.e., V2V links). In other words, a suitable shadowing model dedicated for V2V links has to account for the mobility of both end points and thus, lies beyond the scope of Gudmundson's model. To cope with this problem, an extension of the previous model i.e., the model of Wang *et al.* [17], which generalizes the setting of V2V

TABLE I
MATHEMATICAL NOTATIONS USED IN THE PAPER

Notation	Description
$t_{i,k}$	Vehicle i's sampling instant according to its estimation timeline (e.g., GPS sampling instants).
$\mathbf{x}_{i,k} = (x_{i,k}, y_{i,k})^\dagger$	Vehicle i's 2-D position at time $t_{i,k}$.
$\mathbf{v}_{i,k} = (v^x_{i,k}, v^y_{i,k})^\dagger$	Vehicle i's 2-D velocity at time $t_{i,k}$.
$\boldsymbol{\theta}_{i,k} = (\mathbf{x}_{i,k}, \mathbf{v}_{i,k})^\dagger$	Vehicle i's state vector at time $t_{i,k}$.
$\boldsymbol{\theta}_{j,k_i}$	Vehicle j's state vector at vehicle i's sampling instant $t_{i,k}$. If $j \equiv i$, $\boldsymbol{\theta}_{j,k_i} \equiv \boldsymbol{\theta}_{i,k}$.
$\boldsymbol{\Theta}^k_i$, $\boldsymbol{\Theta}^{k_i}_j$	Sets of all states $\boldsymbol{\theta}_{i,k}$, $\boldsymbol{\theta}_{j,k_i}$ up to (and including) time $t_{i,k}$ respectively.
t_{j,k^*_i}	Vehicle j's latest sampling instant seen by vehicle i at time $t_{i,k}$. If $j \equiv i$, $t_{j,k^*_i} \equiv t_{i,k-1}$.
$\boldsymbol{\theta}_{j,k^*_i}$	Vehicle j's state vector at time t_{j,k^*_i}. For $i \equiv j$, $\boldsymbol{\theta}_{j,k^*_i} \equiv \boldsymbol{\theta}_{i,k-1}$ (at $t_{i,k-1}$).
$\mathcal{N}_{i,k-1:k}$	Set of vehicle i's neighbors in its communication range r_{max} in the time interval $[t_{i,k-1}, t_{i,k})$.
$\mathcal{S}_{i,k} \subset \mathcal{N}_{i,k-1:k}$	Set of vehicle i's reference nodes whose CAMs are selected to feed its fusion engine.
$\boldsymbol{\theta}_{\text{ref},i,k} = \{\boldsymbol{\theta}_{j,k_i}\}_{j\in\mathcal{S}_{i,k}}$	Aggregate state vector of vehicle i's $\lvert\mathcal{S}_{i,k}\rvert$ reference nodes at time $t_{i,k}$ (synchronized state).
$\boldsymbol{\theta}_{\text{ref},i,k^*} = \{\boldsymbol{\theta}_{j,k^*_i}\}_{j\in\mathcal{S}_{i,k}}$	Aggregate state vector of vehicle i's $\lvert\mathcal{S}_{i,k}\rvert$ reference nodes (asynchronous state).
$\mathbf{z}^{\text{GPS}}_{i,k} = (z^x_{i,k}, z^y_{i,k})^\dagger$	Vehicle i's 2-D GPS position at time $t_{i,k}$.
$z^{j\rightarrow}_{i,k}$	Approximated/extrapolated RSSI values at exact filtering time $t_{i,k}$ under some circumstances.
$\mathbf{z}^{\text{ref}\rightarrow}_{i,k} = \{z^{j\rightarrow}_{i,k}\}_{j\in\mathcal{S}_{i,k}}$	Set of vehicle i's RSSI measurements to its reference nodes $\mathcal{S}_{i,k}$ at time $t_{i,k}$.
$\mathbf{z}_{i,k}$	Vehicle i's observation vector at time $t_{i,k}$ (i.e., $\mathbf{z}^{\text{GPS}}_{i,k}$ and/or $\mathbf{z}^{\text{ref}\rightarrow}_{i,k}$).
$\mathbf{Z}^k_i$	Set of all vehicle i's observations up to (and including) time $t_{i,k}$.
$\mathbf{Z}^{k^*_i}_j$	Set of all vehicle j's observations up to (and including) time t_{j,k^*_i}.
$\mathbf{Z}^{k_i}_{\text{ref}} = \{\mathbf{Z}^{k^*_i}_j\}_{j\in\mathcal{S}_{i,k}}$	Set of all observations of vehicle i's reference nodes up to (and including) time t_{j,k^*_i}, $j \in \mathcal{S}_{i,k}$.

links with dual mobility, is chosen to model the correlated shadowing map in this paper. Based on the assumption that the displacements of the two mobile nodes introduce independent but equivalent contributions onto correlation coefficients, the normalized joint ACF when both the Tx and the Rx are in motion can be approximated by the product of the two normalized ACFs when either the Tx or the Rx moves [17], as follows:

$$\begin{aligned} &R_{\text{Sh}}(\Delta\mathbf{x}_t, \Delta\mathbf{x}_r) = \sigma^2_{\text{Sh}} r_{\text{Sh}}(\Delta\mathbf{x}_t, \Delta\mathbf{x}_r) \\ &= \sigma^2_{\text{Sh}} r_{\text{Sh}}(\Delta\mathbf{x}_t, 0) r_{\text{Sh}}(0, \Delta\mathbf{x}_r) \\ &= \sigma^2_{\text{Sh}} \exp\left(-\frac{\|\Delta\mathbf{x}_t\|}{d^{\text{Sh}}_{\text{cor}}}\log 2\right)\exp\left(-\frac{\|\Delta\mathbf{x}_r\|}{d^{\text{Sh}}_{\text{cor}}}\log 2\right) \\ &= \sigma^2_{\text{Sh}} \exp\left(-\frac{v_t + v_r}{d^{\text{Sh}}_{\text{cor}}}\tau\log 2\right) = \sigma^2_{\text{Sh}} r_{\text{Sh}}(\tau) = R_{\text{Sh}}(\tau), \end{aligned} \tag{6}$$

where $\Delta\mathbf{x}_t = (\Delta x_t, \Delta y_t)^\dagger$ and $\Delta\mathbf{x}_r = (\Delta x_r, \Delta y_r)^\dagger$ represent the 2-D displacements of the Tx and the Rx respectively within a time interval τ.

The correlation coefficient R_{Sh} can also be represented as a function of the time lag τ given the knowledge of Tx's and Rx's speeds i.e., v_t and v_r, respectively. Since the spatial joint correlation property of the V2V shadowing is characterized, given both Tx's and Rx's 2-D locations as inputs variables (i.e., $\mathbf{x}_t = (x_t, y_t)^\dagger$ and $\mathbf{x}_r = (x_r, y_r)^\dagger$ respectively), we can simply generate a 4-D spatially correlated shadowing map $\hat{s}(\mathbf{x}_t, \mathbf{x}_r)$ for mobile transceivers by using the SOS-based joint shadowing model in [17]. From (6), one can notice that the joint ACF is now affected by mobility on both extremities of the link, in compliance with generic V2V shadowing needs.

IV. Mitigation of Observation Noise Correlations

A. Signal Level Mitigation

1) Estimation of Cross-Measurement Correlations: This technique relies on the intuition that the knowledge of cross-correlations between the components of the measurement vector provides relevant information to CP [14]. Recall that, although the x-to-y correlation in GPS position is commonly assumed to be null, the cross-correlations between links' fading measurements are accounted in the 4-D shadowing map and can be determined. More particularly, an "ego" vehicle can infer from its "ego" position and the constellation of its "virtual anchors" the correlations between links' fading measurements. From the aforementioned 4-D correlated shadowing model, we therefore derive the cross-correlation between two separate links $a = (i \rightarrow j)$ and $b = (l \rightarrow m)$ as follows:

$$R_{\text{Sh}}(a,b) = \sigma^2_{\text{Sh}} \exp\left(-\frac{\|\mathbf{x}_i - \mathbf{x}_l\| + \|\mathbf{x}_j - \mathbf{x}_m\|}{d^{\text{Sh}}_{\text{cor}}}\log 2\right), \tag{7}$$

where $\|\mathbf{x}_i - \mathbf{x}_l\|$ and $\|\mathbf{x}_j - \mathbf{x}_m\|$ are the Euclidean distances between the transmitters i, l and between the receivers j, m respectively.

For illustration, consider a simplified example where the "ego" car i moving at speed v_i collects three asynchronous RSSI readings with respect to the three neighbors 1, 2, and 3 during the time interval ΔT (e.g., every 100 ms or equivalently, at the fusion rate of 10 Hz). The covariance matrix for the shadowing experienced over these three links is thus inferred from (7) as:

$$\begin{aligned} &\mathbf{R}_{\text{Sh}}(1,2,3 \rightarrow i) \\ &= \begin{pmatrix} \sigma^2_{\text{Sh}} & R_{\text{Sh}}(1,2 \rightarrow i) & R_{\text{Sh}}(1,3 \rightarrow i) \\ R_{\text{Sh}}(2,1 \rightarrow i) & \sigma^2_{\text{Sh}} & R_{\text{Sh}}(2,3 \rightarrow i) \\ R_{\text{Sh}}(3,1 \rightarrow i) & R_{\text{Sh}}(3,2 \rightarrow i) & \sigma^2_{\text{Sh}} \end{pmatrix}, \end{aligned} \tag{8}$$

with

$$\begin{aligned} R_{\text{Sh}}(j,l \rightarrow i) &= \sigma^2_{\text{Sh}} \exp\left(-\frac{\|\mathbf{x}_j - \mathbf{x}_l\| + v_i|t_j - t_l|}{d^{\text{Sh}}_{\text{cor}}}\log 2\right), \\ &\quad j,l \in \{1,2,3\}, \end{aligned} \tag{9}$$

where t_j and t_l represent the time instants at which vehicle i receives the CAMs from its neighbors j and l, respectively. Note that (9) is deduced after applying (7) to a pair of links that has a common end point (i.e., "ego" vehicle i). As vehicle i collects data while moving, cross-link correlation depends on the traveling distance between two corresponding CAMs. Hence, this distance varies from one pair of links to the others. In practice, the true positions (e.g., $\mathbf{x}_j$, $\mathbf{x}_l$ in (7)) cannot be perfectly known. Accordingly, a possible and reasonable approximation $\widehat{R}_{\text{Sh}}(j, l \rightarrow i)$, $j, l \in \{1, 2, 3\}$ leading to $\widehat{\mathbf{R}}_{\text{Sh}}(1, 2, 3 \rightarrow i)$ can be estimated as a function of the estimated positions $\hat{\mathbf{x}}_j$, $\hat{\mathbf{x}}_l$, $j, l \in \{1, 2, 3\}$, which are included in/derived from the received CAM payloads in this example. In practice, when the "ego" vehicle has more reference neighbors, the generalization is straightforward.

2) Differential Measurement (DM): In the literature, there exists a couple of techniques to deal with correlated/colored observation noise. One first approach is to augment the state with the observation noise components [12], [15]. However, this causes a singular measurement noise covariance, which often results in numerical problems [15]. Hence, we concentrate in our work on the second option, referred to as differential measurement (DM). As suggested by its name, the key idea is to whiten the noise by subtracting the correlated part. This problem is solved by building a noise prediction model (from its correlation properties). Being both characterized by the exponential ACF, GPS residual error and shadowing can be predicted by a Gauss-Markov model. In addition, the most dominant mobility pattern in the vehicular context is platooning-like when vehicles move in groups (coordinated or not). Accordingly, their velocities become highly correlated and thus, the memory levels in the prediction model are almost time-invariant in first approximation[5]. For the GPS x- and y-residual errors $n^x_{i,k}$ and $n^y_{i,k}$ respectively, this yields:

$$n^x_{i,k} = \lambda^x_{\text{GPS}} n^x_{i,k-1} + \tilde{n}^x_{i,k}, \quad n^y_{i,k} = \lambda^y_{\text{GPS}} n^y_{i,k-1} + \tilde{n}^y_{i,k}, \tag{10}$$

and for the shadow fading of the link $(j \rightarrow i)$, denoted by $s^{j\rightarrow}_{i,k}$, this leads to:

$$s^{j\rightarrow}_{i,k} = \lambda_{\text{Sh}} s^{j\rightarrow}_{i,k-1} + \tilde{s}^{j\rightarrow}_{i,k}, \tag{11}$$

where $\tilde{n}^x_{i,k}$, $\tilde{n}^y_{i,k}$, and $\tilde{s}^{j\rightarrow}_{i,k}$ are zero mean white Gaussian processes with little variances of $(1 - (\lambda^x_{\text{GPS}})^2)(\sigma^x_{\text{GPS}})^2$, $(1 - (\lambda^y_{\text{GPS}})^2)(\sigma^y_{\text{GPS}})^2$, and $(1 - \lambda^2_{\text{Sh}})\sigma^2_{\text{Sh}}$ respectively.
The memory levels are computed by $\lambda^x_{\text{GPS}} \approx \exp(-v_i \Delta T / d^x_{cor})$, $\lambda^y_{\text{GPS}} \approx \exp(-v_i \Delta T / d^y_{cor})$, and $\lambda_{\text{Sh}} \approx \exp\left(-(v_i + v_j)\Delta T / d^{\text{Sh}}_{cor}\right) \approx \exp\left(-2 v_i \Delta T / d^{\text{Sh}}_{cor}\right)$[6] where ΔT is the measurement sampling period, v_j and v_i the asymptotic mean speeds of the Tx j and the Rx i respectively. In the time interval ΔT till the next fusion time k, the "ego" car i communicates with its set $\mathcal{N}_{\bar{\bar{i}},k-1:k}$ of "virtual" anchors whose cardinality is denoted by $\bar{\bar{N}}_{i,k}$. Hence, the prediction model in the vector form is:

$$\mathbf{n}_{i,k} = \boldsymbol{\lambda} \mathbf{n}_{i,k-1} + \tilde{\mathbf{n}}_{i,k}, \tag{12}$$

where $\boldsymbol{\lambda} = \text{diag}(\lambda^x_{\text{GPS}}, \lambda^y_{\text{GPS}}, \ldots, \lambda_{\text{Sh}}, \ldots)$, $\boldsymbol{\lambda} : \mathbb{R}^{\bar{\bar{N}}_{i,k}+2} \rightarrow \mathbb{R}^{\bar{\bar{N}}_{i,k}+2}$ represents the diagonal memory matrix, $\mathbf{n}_{i,k} = (n^x_{i,k}, n^y_{i,k}, \ldots, s^{j\rightarrow}_{i,k}, \ldots)^\dagger \in \mathbb{R}^{\bar{\bar{N}}_{i,k}+2}$ the observation noise vector, and finally $\tilde{\mathbf{n}}_{i,k} = (\tilde{n}^x_{i,k}, \tilde{n}^y_{i,k}, \ldots, \tilde{s}^{j\rightarrow}_{i,k}, \ldots)^\dagger \in \mathbb{R}^{\bar{\bar{N}}_{i,k}+2}$ the whitened noise vector.
Now the auxiliary measurement $\tilde{\mathbf{z}}_{i,k}$ can be expressed as:

$$\tilde{\mathbf{z}}_{i,k} = \mathbf{z}_{i,k} - \boldsymbol{\lambda} \mathbf{z}_{i,k-1} = \tilde{\mathbf{h}}\left(\boldsymbol{\theta}_{i,k}, \boldsymbol{\theta}_{\text{ref},k_i}\right) + \tilde{\mathbf{n}}_{i,k}, \tag{13}$$

with

$$\tilde{\mathbf{h}}\left(\boldsymbol{\theta}_{i,k}, \boldsymbol{\theta}_{\text{ref},k_i}\right) = \mathbf{h}\left(\boldsymbol{\theta}_{i,k}, \boldsymbol{\theta}_{\text{ref},k_i}\right) - \boldsymbol{\lambda} \mathbf{h}\left(\boldsymbol{\theta}_{i,k-1}, \boldsymbol{\theta}_{\text{ref},k_i-1}\right),$$

and

$$\tilde{\mathbf{n}}_{i,k} = \mathbf{n}_{i,k} - \boldsymbol{\lambda} \mathbf{n}_{i,k-1},$$

where $\boldsymbol{\theta}_{i,k} \in \mathbb{R}^{n_{\boldsymbol{\theta}}}$, $\boldsymbol{\theta}_{\text{ref},k_i} \in \mathbb{R}^{\bar{\bar{N}}_{i,k} \times n_{\boldsymbol{\theta}}}$ are the state vector of "ego" vehicle i and the aggregate state vector of its cooperative neighbors as "virtual anchors" (i.e., the set $\mathcal{N}_{i,k-1:k}$) respectively, $n_{\boldsymbol{\theta}}$ the dimension of the state vector $\boldsymbol{\theta}_{i,k}$, $\mathbf{z}_{i,k} = (x_{i,k}, y_{i,k}, \ldots, z^{j\rightarrow}_{i,k}, \ldots)^\dagger \in \mathbb{R}^{\bar{\bar{N}}_{i,k}+2}$ the aggregate measurement vector, $\tilde{\mathbf{h}} : \mathbb{R}^{n_{\boldsymbol{\theta}}} \times \mathbb{R}^{\bar{\bar{N}}_{i,k} \times n_{\boldsymbol{\theta}}} \rightarrow \mathbb{R}^{\bar{\bar{N}}_{i,k}+2}$ the corresponding model vector for the new measurement vector $\tilde{\mathbf{z}}_{i,k} \in \mathbb{R}^{\bar{\bar{N}}_{i,k}+2}$, and $\tilde{\mathbf{n}}_{i,k} \in \mathbb{R}^{\bar{\bar{N}}_{i,k}+2}$ the prediction noise vector, which is assumed white with a diagonal covariance matrix but cross-correlated with the process noise [12], [15], although this cross-correlation can be neglected at the price of marginal accuracy degradation [12].

Accordingly, our new equivalent observation model can now be written in the same form as (13). Note that contrarily to our proposal, the initial differential measurement technique relies on a new measurement $\tilde{\mathbf{z}}_{i,k} = \mathbf{z}_{i,k+1} - \boldsymbol{\lambda} \mathbf{z}_{i,k}$, which uses the future measurement $\mathbf{z}_{i,k+1}$ as equivalent to 1-lag smoothing [15], thus likely yielding better accuracy gains. Nevertheless, it is inappropriate for real-time tracking in high-mobility contexts such as VANETs.

In addition, in realistic settings, the use of random CAM transmissions introduces specific challenges that should be accounted carefully. Even in case of periodic CAMs, the transmissions are still random due to a so-called CAM generation time between the instant when CAM generation is triggered and the instant when the CAM is delivered to the networking transport layer [4], as illustrated in Fig. 5. Assume that the CAMs are triggered right after estimating the position, it is possible that the CAM is transmitted and thus received too late with respect to the "ego" estimation time, causing i) a lack of up-to-date CAMs (e.g., time window $k-1$ in Fig. 5) and ii) redundant CAMs afterwards (e.g., time window k, same Fig.). In the former subcase, the solution is to simply exclude this neighbor j from the list of "virtual" anchors since there is no RSSI measurement to j available at the estimation time (i.e., $t_{i,k-1}$). In the latter subcase, it is reasonable to retain

[5]The technique is not limited to highly correlated mobility. In a general case, the memory levels become time-variant i.e., depending on the last known speeds of the participants, leading to prediction noises that are statistically independent but not identically distributed (i.e., varying standard deviation).

[6]We consider here the fusion/filter rate equal to the GPS rate i.e., $1/\Delta T$, therefore, only vehicles that send CAMs at this rate (or higher) can become "virtual anchors". If so, the time interval between two consecutive received CAMs/RSSI readings is more or less ΔT due to random CAM generation time and/or congestion control.

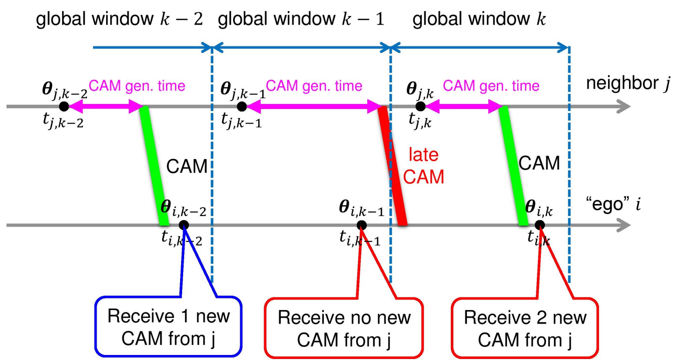

Fig. 5. Impacts of asynchronous position estimates and CAM transmissions on the information fusion.

the latest CAM and to drop the old CAM (e.g., the late CAM in Fig. 5). We observe that this scenario usually occurs as a result of late CAMs. Since there was no observation of j at time $t_{i,k-1}$, the DM can not be performed at time $t_{i,k}$. In other words, a late CAM can prevent its transmitter from becoming a "virtual" anchor up to two "ego" estimates when adopting the DM technique.

B. Adaptive Sampling Mitigation

Unlike signal level mitigation approaches, this protocol level solution eliminates correlations by artificially decreasing the cooperative fusion rate (in comparison with the available rate) without manipulating the observations. For each source of information (i.e., GPS positions and RSSI readings), as the observations are correlated in space with a limited correlation distance d_{cor}, a vehicle moving over a distance D along a straight line can temporally collect up to $1 + \lfloor D/(\gamma d_{\text{cor}}) \rfloor$ uncorrelated measurements where $\gamma \geq 1$ measures the quality of independent instantiations. This simple technique may not be appropriate for GPS collection because GPS correlation distance can be up to hundreds of meters and GPS-assisted dead-reckoning (DR) accumulates errors over time and distance [1]. However, it can be more beneficial for RSSIs due to the short shadowing correlation distance in urban environments (e.g. typically 10–20 m [12], [13], [17]). Moreover, recall that in V2V channels, the decay of the correlation coefficient is affected by both Tx and Rx's displacements (see (6)), hence, Rx vehicles can obtain uncorrelated measurements before completing $d_{\text{cor}}^{\text{Sh}}$ or experience more modest correlation effects at the same distance. Thus, an option is to primarily rely on the DM technique for the correlated GPS sources. The CP is activated to improve the accuracy only if uncorrelated RSSIs are available leading to reduced fusion rates (in comparison with the standalone GPS-based filter rate). One advantage of this hybrid scheme is to cut down on computations by avoiding unnecessary fusion steps while maintaining an equivalent tracking performance. Another benefit lies in the ability to adopt the first proposed technique (i.e., estimation of cross-link correlations) to minimize the effects of correlated noises or to approach the standard filtering performance with i.i.d noises. Finally, the scenario depicted in Fig. 5 (i.e., late CAMs) are also interestingly supported with this technique. Remarkably, the strategy (and thus, the impact) is similar to that of DM techniques. In other words, one neighbor sending a late CAM cannot be a reference vehicle.

In case of channel congestion, the ETSI Decentralized Congestion Control (DCC) rules recommend to scale the transmission rate down to 2 Hz, what is still higher than the slowest proposed fusion rate (e.g., 1.43 Hz on Fig. 9). Accordingly, we do not expect any negative impact from channel congestion cases. We even claim that the system is perfectly resilient to channel congestion situations, besides its clear advantage in terms of overhead.

C. Integration into the Fusion Framework

1) Resynchronization of Cooperative Information: As available sources of information (i.e., data received from neighboring vehicles and/or on-board device like GPS) are adversely asynchronous in the high speed vehicular context, data resynchronization is then naturally achieved via an early prediction step applied to both "ego" and neighboring position estimates [6]. Thus, in compliance with PF as core fusion engine, the prediction step made by vehicle i can be simply formulated as follows:

$$\begin{aligned}
&\boldsymbol{\theta}_{j,k_i}^{(p)} \sim p\left(\boldsymbol{\theta}_{j,k_i} \middle| \boldsymbol{\theta}_{j,k_i^*}^{(p)}\right), && w_{j,k_i|k_i^*}^{(p)} = w_{j,k_i^*}^{(p)},\\
&j \in \{i\} \cup \mathcal{N}_{i,k-1:k}, && p = 1, \ldots, N_p,
\end{aligned}$$

where $\{\boldsymbol{\theta}_{j,k_i}^{(p)}, w_{j,k_i|k_i^*}^{(p)}\}_{p=1}^{N_p}$ indicates the predicted N_p-particle cloud drawn from the dynamic/mobility model (i.e., from (1a)). Intuitively, it yields (See again Fig. 4):

$$\begin{aligned}
&\boldsymbol{\theta}_{j,k_i}^{(p)} = \mathbf{F}_j(t_{i,k} - t_{j,k_i^*})\boldsymbol{\theta}_{j,k_i^*}^{(p)} + \mathbf{f}_j(t_{i,k} - t_{j,k_i^*}) +\\
&\mathbf{G}_j(t_{i,k} - t_{j,k_i^*})\mathbf{w}_{j,k}^{(p)}, \quad j \in \{i\} \cup \mathcal{N}_{j,k-1:k}, \quad p = 1, \ldots, N_p.
\end{aligned}$$

So far, we have just re-synchronized both "ego" and neighboring position estimates. But RSSI readings are also not perfectly synchronous (e.g., the CAM broadcasts may occur at different rates and/or they can be event-driven) with estimation times. In case of highly correlated velocities (e.g., vehicles forming a platoon on a highway), relative distances are expected to remain quite stable in the medium term, and hence, so are the RSSI measurements (at least, in average) [6]. For this reason, not all the neighbors can become "virtual" anchors for CP with respect to a given "ego" car. This paper only concentrates on selecting neighboring vehicles that lead to exploitable RSSIs at the fusion time (i.e., according to a short-term stable V2V distance criterion). In most common platooning cases, stable V2V distances between vehicles are usually observable, leading to the possibility of exhaustive cooperation.

2) Overall Fusion Implementation: As the observation model of interest linking the state vector to the measurements is non-linear here (e.g., See (4)), filtering strategies relying on numerical approximations (e.g., PF) are expected to outperform that based on linear approximations (e.g., Extended Kalman Filters) in terms of accuracy, at the price of higher

[7]Note that when employing decreased fusion rate the cross-link correlation information (in terms of covariance matrix) helps to better characterize the distribution of the measurement noise vector (i.e., $p(\bar{\mathbf{z}}_{i,k}^{\text{ref}\rightarrow}|\boldsymbol{\theta}_{i,k}^{(p)}, \boldsymbol{\theta}_{\text{ref},i,k}^{(p)})$).

Algorithm 1 PF in CP engine (iteration k, "ego" vehicle i)

1: **Collection of CAMs:** Receive CAMs from the set $\mathcal{N}_{i,k-1:k}$ of the neighbors, read the RSSI values, extract the neighboring particle clouds $\{\boldsymbol{\theta}^{(p)}_{j,k^*_i}, w^{(p)}_{j,k^*_i}\}_{p=1}^{N_p}$, $j \in \mathcal{N}_{i,k-1:k}$.

2: **Data Resynchronization:** Perform prediction at the "ego" estimation instance k (i.e., the global time $t_{i,k}$)

$$\begin{aligned} &\boldsymbol{\theta}^{(p)}_{j,k_i} \sim p\left(\boldsymbol{\theta}_{j,k_i}\middle|\boldsymbol{\theta}^{(p)}_{j,k^*_i}\right), && w^{(p)}_{j,k_i|k^*_i} = w^{(p)}_{j,k^*_i} = 1/N_p, \\ &j \in \{i\} \cup \mathcal{N}_{i,k-1:k}, && p = 1, \ldots, N_p, \end{aligned}$$

build the LDM of all the neighbors as the first output

$$\hat{\boldsymbol{\theta}}_{j,k_i} \approx \sum_{p=1}^{N_p} w^{(p)}_{j,k_i|k^*_i} \boldsymbol{\theta}^{(p)}_{j,k_i} = \frac{1}{N_p} \sum_{p=1}^{N_p} \boldsymbol{\theta}^{(p)}_{j,k_i}, \quad j \in \mathcal{N}_{i,k-1:k}.$$

3: **Mitigation of Noise Correlations:** Select the subset $\mathcal{S}_{i,k} \subset \mathcal{N}_{i,k-1:k}$ of appropriate links. Manipulate the measurements (and the corresponding observation model)

$$\begin{aligned} \bar{\mathbf{z}}_{i,k} &= \left[\left(\bar{\mathbf{z}}^{\text{GPS}}_{i,k}\right)^\dagger, \left(\bar{\mathbf{z}}^{\text{ref}\rightarrow}_{i,k}\right)^\dagger\right]^\dagger \\ &= \begin{cases} \left[\left(\tilde{\mathbf{z}}^{\text{GPS}}_{i,k}\right)^\dagger, \left(\tilde{\mathbf{z}}^{\text{ref}\rightarrow}_{i,k}\right)^\dagger\right]^\dagger, & \text{if differential measurement,} \\ \left[\left(\tilde{\mathbf{z}}^{\text{GPS}}_{i,k}\right)^\dagger, -\right]^\dagger, & \text{if non-fusion instant } k, \\ \left[\left(\tilde{\mathbf{z}}^{\text{GPS}}_{i,k}\right)^\dagger, \left(\mathbf{z}^{\text{ref}\rightarrow}_{i,k}\right)^\dagger\right]^\dagger, & \text{if fusion instant } k, \end{cases} \end{aligned}$$

where $\tilde{\mathbf{z}}^{\text{GPS}}_{i,k}$ and $\tilde{\mathbf{z}}^{\text{ref}\rightarrow}_{i,k}$ are the differential 2-D GPS position and RSSI vector respectively, $\mathbf{z}^{\text{ref}\rightarrow}_{i,k}$ is the standard RSSI vector.

4: **Observation Update:** Calculate the new weights according to the likelihood[7] (by using the proposal distribution in (16))

$$\begin{aligned} w^{(p)}_{i,k} &\propto p\left(\bar{\mathbf{z}}_{i,k}\middle|\boldsymbol{\theta}^{(p)}_{i,k}, \boldsymbol{\theta}^{(p)}_{\text{ref},i,k}\right) \\ &= p\left(\bar{\mathbf{z}}^{\text{GPS}}_{i,k}\middle|\boldsymbol{\theta}^{(p)}_{i,k}\right) p\left(\bar{\mathbf{z}}^{\text{ref}\rightarrow}_{i,k}\middle|\boldsymbol{\theta}^{(p)}_{i,k}, \boldsymbol{\theta}^{(p)}_{\text{ref},i,k}\right), \quad p = 1, \ldots, N_p, \end{aligned}$$

and normalize them to sum to unity. Then compute the approximate mean as the second filter/fusion output

$$\hat{\boldsymbol{\theta}}_{i,k} \approx \sum_{p=1}^{N_p} w^{(p)}_{i,k} \boldsymbol{\theta}^{(p)}_{i,k}.$$

5: **Resampling**

6: **Broadcast**

computational load [15], [24], [34]. However, in the vehicular context, the relative extra-cost to supply adequate powerful hardware and software capabilities looks still reasonable (comparing with the cost of the whole car). The key idea of PF is to approximately represent the *a posteriori* density function[8] by a set of random samples with associated weights and to compute estimates based on these samples and weights [24], [34]. Accordingly, we approximate the optimal solution:

$$\hat{\boldsymbol{\theta}}_{i,k} = \int \boldsymbol{\theta}_{i,k} p\big(\boldsymbol{\theta}_{i,k}, \boldsymbol{\theta}_{\text{ref},i,k}\big|\mathbf{Z}^k_i, \mathbf{Z}^{k_i}_{\text{ref}}\big) d\boldsymbol{\theta}_{i,k} d\boldsymbol{\theta}_{\text{ref},i,k}, \quad (14)$$

by

$$\hat{\boldsymbol{\theta}}_{i,k} \approx \sum_{p=1}^{N_p} w^{(p)}_{i,k} \boldsymbol{\theta}^{(p)}_{i,k}, \quad (15)$$

where $\{\boldsymbol{\theta}^{(p)}_{i,k}\}_{p=1}^{N_p}$ is a set of particles (samples of the state vector) with associated weights $\{w^{(p)}_{i,k}\}_{p=1}^{N_p}$, $w^{(p)}_{i,k} \propto p(\boldsymbol{\theta}^{(p)}_{i,k}, \boldsymbol{\theta}^{(p)}_{\text{ref},i,k}|\mathbf{Z}^k_i, \mathbf{Z}^{k_i}_{\text{ref}})/q(\boldsymbol{\theta}^{(p)}_{i,k}, \boldsymbol{\theta}^{(p)}_{\text{ref},i,k}|\boldsymbol{\theta}^{(p)}_{i,k-1}, \boldsymbol{\theta}^{(p)}_{\text{ref},i,k^*}, \mathbf{z}_{i,k})$ with the (important) distribution $q(\cdot)$.

A classical and intuitive choice for computing these weights involves the measurement likelihood function [24], [34]. It can be solved by choosing the following distribution:

$$\begin{aligned} &q\left(\boldsymbol{\theta}_{i,k}, \boldsymbol{\theta}_{\text{ref},i,k}\middle|\boldsymbol{\theta}^{(p)}_{i,k-1}, \boldsymbol{\theta}^{(p)}_{\text{ref},i,k^*}, \mathbf{z}_{i,k}\right) = p\left(\boldsymbol{\theta}_{i,k}\middle|\boldsymbol{\theta}^{(p)}_{i,k-1}\right) \\ &\times p\left(\boldsymbol{\theta}_{\text{ref},i,k}\middle|\boldsymbol{\theta}^{(p)}_{\text{ref},i,k^*}\right) \\ &= p\left(\boldsymbol{\theta}_{i,k}\middle|\boldsymbol{\theta}^{(p)}_{i,k-1}\right) \prod_{j \in \mathcal{S}_{i,k}} p\left(\boldsymbol{\theta}_{j,k_i}\middle|\boldsymbol{\theta}^{(p)}_{j,k^*_i}\right). \end{aligned} \quad (16)$$

We then propose to apply the PF described in Algorithm 1 as the core filter/fusion engine of our CP framework.

V. Performance Evaluation

A. Simulation Settings and Scenarios

1) Gauss-Markov Mobility Model: We consider a stochastic mobility model suitable for the vehicular context called modified Gauss-Markov prediction model (GMM). It describes well the correlated velocity of the vehicle as a time-correlated process and enables good predictions of the vehicle's position and velocity [25], while remaining still analytically tractable[9]. In discrete time, the predicted velocity in 2-D is computed based on its previous value and a Gaussian i.i.d process [6], [25], as follows:

$$v^{(\cdot)}_{i,k+1} = \alpha v^{(\cdot)}_{i,k} + (1-\alpha)\mu^{(\cdot)}_i + \Delta T \sqrt{1-\alpha^2} w^{(\cdot)}_{i,k}, \quad (17)$$

where $(\cdot)$ can be either x- or y-coordinate, α is the memory level, ΔT the time step, $\mu^{(\cdot)}_i$ the asymptotic 1-D mean velocity, and $a^{(\cdot)}_{i,k} = \sqrt{1-\alpha^2} w^{(\cdot)}_{i,k}$ the Gaussian i.i.d. 1-D acceleration noise. Note that vehicles usually move along the lanes on the roads. Accordingly, the uncertainty along the road direction is much higher than that along the orthogonal dimension [8].

Also note that we use this mobility model to perform the predictions of both "ego" and neighbors' estimated locations and resynchronize related data before fusion (See step 2 of Algorithm 1).

2) Correlated Observation Generation: As the spatial/temporal correlation properties and models have been investigated in Subsection III-B, we herein recall the SOS-based approach to generate the corresponding processes in our simulations. Given the true 2-D GPS receiver's position $\mathbf{x} = (x, y)^\dagger$, the 2-D correlated GPS x- and y-error maps $\hat{n}^x(\mathbf{x})$, $\hat{n}^y(\mathbf{x})$ are drawn as follows:

$$\hat{n}^{(\cdot)}(\mathbf{x}) = \sigma^{(\cdot)}_{\text{GPS}} \sqrt{\frac{2}{N}} \sum_{n=1}^{N} \cos\left(2\pi \mathbf{f}^{(\cdot)\dagger}_n \mathbf{x} + \psi^{(\cdot)}_n\right), \quad (18)$$

where $(\cdot)$ can be either x- or y-coordinate, $\{\psi^{(\cdot)}_n t\}_{n=1}^N$ represents a set of random phase terms uniformly distributed over $[0, 2\pi)$, $\{\mathbf{f}^{(\cdot)}_n\}_{n=1}^N = \{f^{(\cdot)}_{x,n}, f^{(\cdot)}_{y,n}\}_{n=1}^N$ the 2-D random discrete spatial frequencies that can be generated according to a given

[8]In our proof-of-concept validations, CAMs encapsulate the particles cloud to account for local estimates uncertainty, what could result in prohibitive overhead under current standard specifications. This issue, which does not fall in the paper scope, has been investigated in [35] without contradicting the first findings exposed herein.

[9]The evaluation of this work over real or synthetic mobility traces are left to future work (See VI).

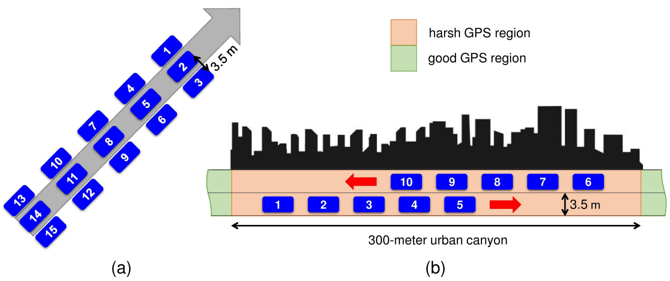

Fig. 6. Topology of the evaluated VANETs and related attributes in (a) highway/tunnel and (b) urban canyon scenarios.

joint pdf $p(\mathbf{f}^{(\cdot)})$ related to the 2-D power spectral density (PSD) of the shadowing process (i.e., performing 2-D Fourier transformation on (3)), by using a frequency sampling Monte Carlo method (MCM), as detailed in [27].

Regarding the V2V RSSI measurements, with knowledge of both Tx's 2-D position $\mathbf{x}_t = (x_t, y_t)^\dagger$ and Rx's position $\mathbf{x}_r = (x_r, y_r)^\dagger$, the 4-D spatially correlated shadowing map $\hat{s}(\mathbf{x}_t, \mathbf{x}_r)$ is then generated using [17], as follows:

$$\hat{s}(\mathbf{x}_t, \mathbf{x}_r) = \sigma_{\text{Sh}} \sqrt{\frac{2}{N}} \sum_{n=1}^{N} \cos\left(2\pi \mathbf{f}_n^\dagger \left(\mathbf{x}_t^\dagger, \mathbf{x}_r^\dagger\right)^\dagger + \phi_n\right), \quad (19)$$

where $\{\phi_n\}_{n=1}^N$ are random phase terms uniformly distributed over $[0, 2\pi)$, $\{\mathbf{f}_n\}_{n=1}^N = \{\mathbf{f}_n^t, \mathbf{f}_n^r\}_{n=1}^N = \{f_{x,n}^t, f_{y,n}^t, f_{x,n}^r, f_{y,n}^r\}_{n=1}^N$ 4-D random spatial frequencies generated according to a given joint pdf related to the 4-D PSD of the shadowing process (i.e., performing 4-D Fourier transformation on (6)) through MCM, again like in [17], [27].

Moreover, following [17], we consider the shadowing symmetric property in V2V networks, leading to identical fluctuations on both sides of the link i.e., $s(\mathbf{x}_t, \mathbf{x}_r) = s(\mathbf{x}_r, \mathbf{x}_t)$ due to a common channel propagation path. Accordingly, we "symmetrically" manipulate the aforementioned 4-D spacial frequencies and phases through symmetric MCM.

3) Evaluation Scenarios and Related Simulation Settings: In this paper, our evaluation framework is based on MATLAB simulations, which are more flexible and suitable in the specific wireless localization context (estimation algorithms) than network simulators, more devoted to communication aspects. Our Monte Carlo trials are performed in 3 representative environments and scenarios, namely the highway, the urban city and the tunnel, which naturally provide contrasted vehicular propagation channels and mobility conditions. In particular, as illustrated in Fig 6, we firstly model a three-lane highway (of most common kind in Europe), where fifteen IEEE 802.11p-connected cars are driving steadily (in the same north-east direction) at the average speed of 110 km/h (i.e., $\approx$ 30 m/s) for 3,000 meters. The latter vehicles establish a pure VANET and can benefit from relatively favorable GPS signals due to the open sky operating environment. Secondly, we focus on a more critical GPS-denied scenario. Specifically, the aforementioned VANET goes through a 3-lane straight portion of urban tunnel at the average speed of 50 km/h (i.e., $\approx$ 15 m/s) for 1,500 meters. Finally, we consider a short urban canyon of 300 meters in the form of a 2-lane narrow street with opposite traffic directions (i.e., one direction per lane).

In the previous scenarios, we systematically consider a group of 15 vehicles, focusing our analysis on a segment of the entire vehicles flow. CAMs could indeed be received up to practical transmission ranges of 1,000 m. However we consider a nominal selective CP scheme that incorporates only the messages from its nearest neighbors like in [6], [33]. Accordingly, simulating 15 vehicles is enough to avoid border effects or artifacts, while preserving the generality of the obtained CP results. The related mobility and traffic model parameters are summarized in Table II.

TABLE II
MOBILITY MODEL AND TRAFFIC PARAMETERS

Parameter	Highway	Urban Canyon	Tunnel
Memory level α	0.95		
Asym. mean speed $\|\boldsymbol{\mu}_i\|$	30 [m/s]	15 [m/s]	15 [m/s]
Std. of the noise σ_i^d	1 [m/s^2]	3 [m/s^2]	1 [m/s^2]
Std. of the noise σ_i^o	0.1 [m/s^2]	0.95 [m/s^2]	0.1 [m/s^2]
Sampling period ΔT	0.1 [s]		
Simulation time	100 [s]	12 [s]	100 [s]
Number of lanes	3	2	3
Traffic direction(s)	1 (Common)	2 (Opposite)	1 (Common)
Simulated track length	3,000 [m]	300 [m]	1,500 [m]

Besides, depending on each scenario configuration and on generated mobility traces, conditional models are applied in terms of both GPS and V2V RSSI observations based on measurement-based parameters from the recent literature (whenever available), as reported in Table III.

As for the CAM transmission policy, we assume that each vehicle periodically broadcasts its position every 100 ms corresponding to the critical CAM rate of 10 Hz (equal to the "core" BSM rate in the U.S. [5]) for several reasons: first, this assumption is valid on high speed mobility scenarios (e.g., highways) where dynamic related conditions in [4] are triggered to get critical rates; second, the positions can be collected up to 10 Hz thanks to the high-rate GPS receivers; third, we are interested in how the cooperative information can improve the CP accuracy[10]. Besides, the random CAM generation time between the instant at which CAM generation is triggered (GPS position is sampled) and the instant at which the message is delivered to the transport layer is uniformly drawn in the interval $[0, 50]$ ms (complying with [4]) to alleviate simultaneous transmissions and temporal correlated packet collisions. Besides mobility and propagation considerations, Table IV summarizes the remaining common simulation parameters and settings used in the three simulated scenarios, regarding the CAM transmission rate and times, the GPS refresh rate and the generation of correlated processes.

In our comparative study, we consider two different positioning contexts i.e., the filtered standalone GPS (non-CP solution) and the exhaustively fused GPS+DSRC (CP solution) both running at the filter/fusion rate of 10 Hz (i.e., the rate of GPS refreshment and critical CAM generation). First, we analyze them in unrealistic i.i.d noise environments, which

[10]Injecting too many packets to the channel with limited capacity causes traffic congestion. As this work is positioning-oriented, communication behavior is not examined to the fullest but left for further studies.

TABLE III
CORRELATED OBSERVATION ERROR/DISPERSION MODEL PARAMETERS

Modality	Parameter	Urban Canyon	Tunnel[a]	Highway
V2V RSSI	n_p	low (1.6 [36])	id.	low (1.9 [37])
	σ_{dB}	large (3.4 dB [36])	id.	medium (2.5 dB [37])
	$d_{\text{cor}}^{\text{Sh}}$	very short (3 m [23])	id.	large (20 m [23])
GPS position	σ_{GPS}	large (10–30 m [2], [9])	N/A (no GPS)	medium (3-10 m [2], [8], [9])
	$d_{\text{cor}}^{\text{GPS}}$	medium/building-dependent (50–100 m)	N/A (no GPS)	very large/open sky (100–500 m)

[a] In lack of representative figure/information available for this scenario in the recent literature (to the best of our knowledge), we assume in first approximation i) rather similar conditions than that of the Urban canyon scenario (due to the confined propagation medium, and rather similar conditions in terms of car density and speed) but ii) no GPS at all and a larger number of lanes having the same traffic direction (See Section II).

TABLE IV
OTHER COMMON HIGH-LEVEL SIMULATION PARAMETERS.

Parameter	Description
GPS refresh rate	10 [Hz]
CAM rate	10 [Hz] (critical) [4], [5]
CAM generation time	$\mathcal{U}(0, 50)$ [ms] [4]
No. of cosines N for models in (18), (19)	100–1000 [17], [27]
No. of particles N_p in Algorithm 1	1000

are widely considered in literature so far as two benchmark approaches. Second, we test them under realistic correlated conditions. Last, we add two proposed methods to decorrelate the noises i.e., differential measurement (DM) and decreased fusion rate (or adaptive sampling). More specifically, we obtain three solutions including the filtered GPS with DM (at 10 Hz), the exhaustively fused GPS+DSRC with DM (at 10 Hz), and the hybrid fused GPS+DSRC incorporating the filtered GPS with DM at 10 Hz and DSRC at lower rate.

Regarding the hybrid option, the RSSIs are collected over each traveling distance equivalent to the shadowing correlation length. Thus, the normalized joint ACF (i.e., (6)) reduces by $1/2 \times 1/2 = 1/4$ due to dual mobility at both "ego" and neighboring cars. Mathematically, considering 10-Hz refresh rate of the filter/fusion, the decreased fusion rate can be computed by:

$$r_x = 10 \left\lceil 10 \frac{-d_{\text{cor}}^{\text{Sh}} \log_2 x}{2v} \right\rceil^{-1}, \tag{20}$$

where r_x [Hz] is the decreased fusion rate aiming at $x\%$ in the normalized joint ACF, and v is the vehicle's average speed. For example, in the highway scenario, 20-m correlation length and 30-m/s speed yield a rate of about 1.43 Hz while in the urban case, 3-m correlation length and 15-m/s speed give a rate of 5 Hz.

Besides, cross-link correlation information is added to the hybrid solution but not with the DM technique, whose differential noise vector is by design white (i.e., having diagonal covariance matrix).

B. Performance Metrics

To evaluate the positioning/tracking performance, we first define the positioning error E_i of the "ego" vehicle i. E_i is a random variable which takes sampled value $e_{i,k}$ at time $t_{i,k}$ as follows:

$$e_{i,k} = \|\hat{\mathbf{x}}_{i,k} - \mathbf{x}_{i,k}\|, \tag{21}$$

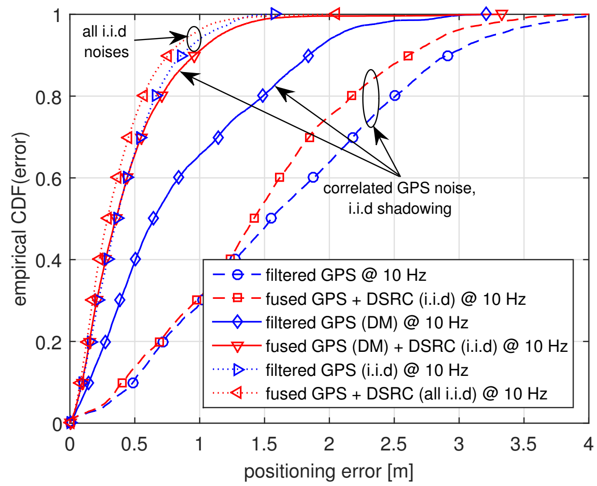

Fig. 7. Positioning performance comparison of different schemes assuming correlated GPS noise and i.i.d shadowing except the two top curves of the all i.i.d cases in the highway scenario.

where $\hat{\mathbf{x}}_{i,k}$ and $\mathbf{x}_{i,k}$ represent respectively the 2-D estimated and true positions of the "ego" car i at time $t_{i,k}$. We are then interested in the empirical cumulative distribution function (CDF) of the positioning error E_i. Said differently, the probability that the positioning error does not exceed a certain threshold can be specified for all threshold values, that is:

$$F(x) = \mathbb{E}_i \left\{ p\left(e_i \leq x\right) \right\}, \tag{22}$$

where the expectation $\mathbb{E}_i\{\cdot\}$ is taken over all the vehicles in the VANET.

We then extract characteristic values of the error statistics, such as the median error (CDF of 50%) or the so-called worst-case (WC) error (arbitrarily defined for a CDF of 90% herein).

C. Numerical Results

1) Highway Scenario: We now analyze the effects of measurement correlation on filtering/fusion performance and evaluate the gains from the proposed techniques by undertaking "step-by-step" investigations. We first consider either GPS noise or shadowing to be correlated (while assuming the other process to be i.i.d.) and ultimately, we assume both processes to be correlated.

a) Testing Scenario of Correlated GPS Noise and i.i.d Shadowing (S1): In this first example, we deal with GPS noise correlation with the DM technique. The results are summarized in Fig. 7 by means of empirical CDFs. As expected, when

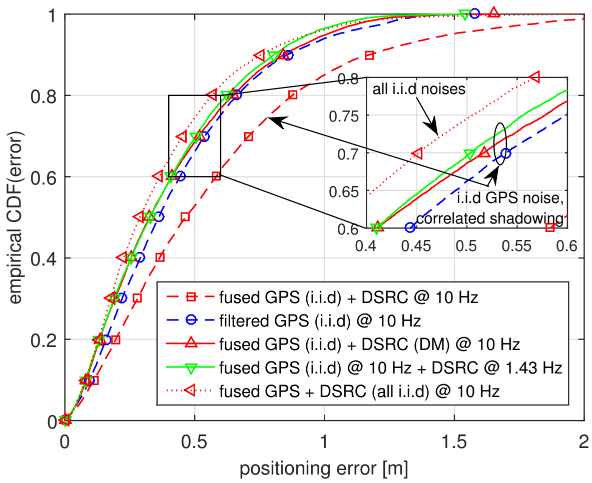

Fig. 8. Positioning performance comparison of different schemes assuming i.i.d GPS noise and correlated shadowing except the top curve of the all i.i.d case in the highway scenario.

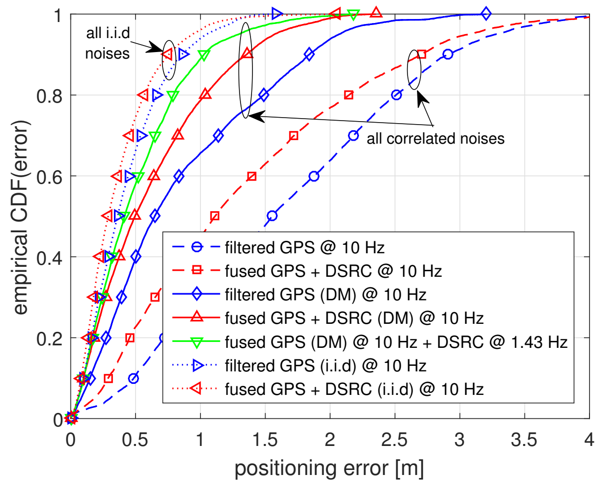

Fig. 9. Positioning comparison of different schemes assuming correlated GPS noise and correlated shadowing except the two top curves of the all i.i.d cases in the highway scenario.

the GPS position noise is decorrelated by DM, huge accuracy improvements are observed in both non-CP (i.e., single GPS) and CP (i.e., GPS+DSRC) solutions. More specifically, for the filtered standalone GPS, the position estimates accounting for the noise correlation experience significant relative drops by 58% in median error and 37% in WC error from those neglecting the noise correlation. Similarly, massive relative decreases by 75% in median error and 63% in WC error are noticeable after integrating the DM technique in the exhaustively fused GPS+DSRC. On the other hand, Fig. 7 confirms the advantage of CP over non-CP regardless of noise decorrelation. A closer look reveals that the filtered GPS without DM draws less significant accuracy gains from the DSRC than that with DM as correlated noise is a threat to the effectiveness of data fusion. Besides, the positioning performance delivered by the filtered GPS after whitening the correlated noise remains quite below that achieved in the i.i.d noise case. Three main reasons can be invoked: first, error transfer from the previous estimate to the current estimate via the new observation model (i.e., $\tilde{\mathbf{h}}(\cdot)$ in (13)) after performing DM between the current and the previous measurements; second, model mismatch (i.e., simulating finite SOS based on an exponential ACF vs. assuming first order Gauss-Markov noise prediction model); third, possible cross-correlation between the whitened measurement noise and the process noise. Nevertheless, this problem can be solved by enabling CP (i.e., exhaustively fused GPS (DM) and DSRC), which approaches the i.i.d case, as shown in Fig. 7.

b) Testing Scenario of i.i.d GPS Noise and Correlated Shadowing (S2): In case of correlated shadowing, both DM and decreased fusion rate can be employed for RSSI measurements. Note that when GPS error is assumed i.i.d, the filtered GPS achieves very high accuracy (See the second top curve in Fig. 7). This is challenging to our fusion scheme since RSSI-based positioning is not considered as a high precision solution and as such, may deteriorate the performance [22]. It can be seen clearly from Fig. 8 that the cooperative GPS+DSRC solution neglecting shadowing correlation produces erroneous estimates in comparison with the non-cooperative filtered GPS, confirming that the careless handling of shadowing correlation incurs convergence issues. When the shadowing is decorrelated by either the DM method or by a decreased fusion rate (from 10 Hz to 1.43 Hz), the cooperative GPS+DSRC option now slightly outperforms the standalone filtered GPS and closely approaches the GPS+DSRC fusion option in the i.i.d case. The reason can be understood as follows. In comparison with GPS positions, RSSI measurements with respect to "virtual anchors" can contribute to the positioning performance but to a rather modest extent due to the non-linear relationship between the received power and the state variables. Finally, both extrapolated/approximate RSSI values at the fusion time instant and virtual anchors' uncertainties may alter the positioning performance. In other words, when the accuracy of the filtered GPS remains high enough (e.g., under i.i.d assumption and low GPS noise), there is little room for improvement by fusing with DSRC.

c) Testing Scenario of Correlated GPS Noise and Correlated Shadowing (S3): In this experiment, we let both GPS position noise and shadowing correlated to examine the performance of the proposed algorithms. The results summarized in Fig. 9 are compliant with that of the previous case (S1) for the filtered standalone GPS with/without DM. As we have already noted accuracy improvements from noise decorrelation in the filtered standalone GPS, it is worth verifying how the performance can be further boosted under correlated RSSIs too. The corresponding performance will be seen as a reference. As expected, the cooperative fused GPS+DSRC with DM yields apparent performance improvement (relative drops of 23% in median error and 26% in WC error) over the filtered GPS with DM. However, this scheme does not approach the corresponding i.i.d case as in (S1) (See again Fig. 7) due to the fact that the DM method for RSSIs has the same drawbacks as for GPS positions (as pointed out in (S1)). Hence, differential RSSIs are less beneficial than i.i.d RSSIs in (S1). On the other hand, the hybrid fused GPS+DSRC (i.e., combining the filtered GPS with DM at 10 Hz and

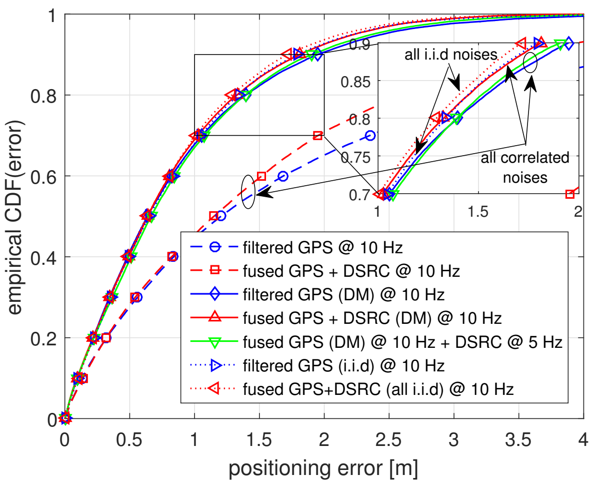

Fig. 10. Positioning performance comparison of different schemes assuming correlated GPS noise and correlated shadowing except the two dotted curves of the all i.i.d cases in the urban canyon scenario.

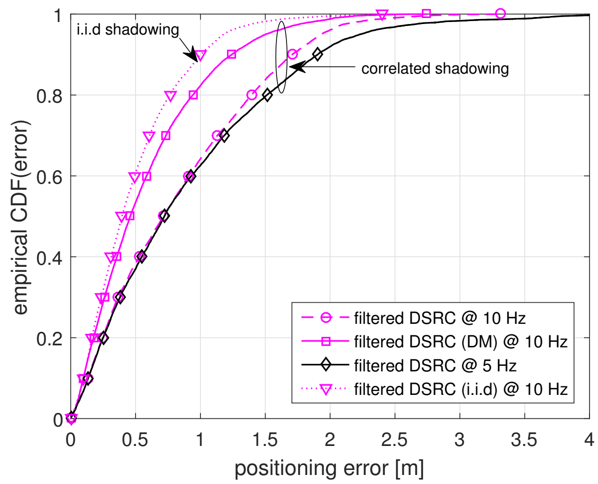

Fig. 11. Positioning performance comparison of different schemes assuming loss of GPS signal and correlated shadowing except the top curve of i.i.d shadowing in the tunnel scenario.

DSRC at 1.43 Hz) enables very favorable positioning results in consideration of collecting temporally uncorrelated RSSI measurements and exploiting the cross-link correlation, thus compensating for the information loss in the fusion model. Quantitatively, the accuracy improvement matches by less than 10% the performance of optimal CP when considered under i.i.d measurements. In comparison with cooperative GPS+DSRC under the same decreased fusion rate as in (S2) (See again Fig. 8), we observe that the hybrid scheme in (S3) suffers from slightly degraded positioning performance due to GPS noise correlation.

2) Urban Canyon Scenario: Just like in the highway environment, we now evaluate the different solutions in the urban canyon scenario. Fig. 10 shows the performance comparison. We note again the adverse effects of correlated noises on the filtering performance (the two dash curves vs. the two dotted curves). From this figure, we also remark that CP provides lower performance gains in comparison with standalone GPS than in the highway scenario. This can be explained as follows. Firstly, the two platoons traveling in opposite directions along the narrow street (i.e., 1 single lane per traffic direction) introduce poorer GDOP conditions that tend to spoil the RSSI-based multilateration result. That can be even more severe since neighboring vehicles (i.e., considered as "virtual anchors") experience equivalent dispersion of their respective positioning errors. Secondly, shadowing in urban environments is usually stronger than on highways, leading to higher observation noise in the fusion filter [13]. Interestingly, the three proposed techniques (i.e., the filtered GPS with DM, the fused GPS+DSRC with DM, and the hybrid fused GPS+DSRC) now approach closely the ideal i.i.d cases. This is due to the specificities of the tested urban canyon scenario. It is commonly admitted that urban canyons belong to the most problematic situations with respect to vehicular localization. We reasonably assume that the vehicles entering the urban canyons from other areas would have preliminary produced rather good state estimates e.g., in open sky areas, along wider avenues or roads with smaller buildings... (See again Fig. 2) [33]. Hence, in the short term, the noise prediction model depending on velocity estimation is beneficial to effectively decorrelate the noises. However, in the long term, larger state errors would appear, thus jeopardizing the prediction and further impairing the accuracy performance in comparison with the i.i.d schemes. This happens in the highway scenario with a simulated track length of 3,000 m but not within our short urban canyon scenario of 300 m since the vehicles soon escape from this canyon. A closer look at Fig. 10 reveals that GPS+DSRC with DM marginally outperforms the hybrid fused GPS+DSRC scheme. This is due to the short correlation length in urban environments (i.e., 3 m in this case). Accordingly, the correlation between two consecutive RSSI measurements becomes weak. Quantitatively, 10-Hz RSSI measurements, 15 m/s mobility, and a 3-m correlation distance would lead to a normalized joint ACF value of 50%, which can already be considered as a successful decorrelation without decreasing further the fusion rate. However, weakly correlated measurements imply new information contained in each new measurement. As a result, reducing the fusion rate leads to miss such information and hence, to lower accuracy.

3) Tunnel Scenario: Finally, we are interested in the even more specific GPS-denied tunnel environment. In this case, we only rely on one single modality, namely RSSI measurements, to perform ad hoc-based multilateration with respect to neighboring vehicles. Fig. 11 shows the performance comparison. Once again, we remark that the DM technique decorrelates the shadowing noises to improve accuracy close to that of the ideal i.i.d case. Considering the filtered DSRC without DM as reference for benchmark purposes, relative accuracy gains of respectively 36% on the median error and 27% in the worst-case (WC) error regime are reported. Moreover, it matches by less than 20% the ideal scheme under i.i.d shadowing. Interestingly, from Fig. 11, we can see that decreasing the fusion rate provides the poorest performance, which is even worse than that of the original filtered DSRC. It can be explained as follows. First, this is again due to very short correlation length, which leads to loose information from naturally decorrelated RSSI measurements while decreasing the fusion rate, as already mentioned in the urban canyon scheme. Secondly, with a 5-Hz RSSI fusion rate, we need to use prediction (i.e., Dead Reckoning) in order to deliver 10-Hz position estimates because of the GPS loss. Thus, the positioning error tends to accumulate more easily over time.

4) Discussion on Practical Context-Aware Correlation Mitigation: We have evaluated our proposed methods in different kinds of environments and scenarios. We have found that the characteristics of the environment, including correlation lengths, mobility patterns, GPS availability... strongly influence how the CP data fusion processes the different input measurements to mitigate the noise correlation. A technique can be very favorable in one environment but may be less effective in the others. Thus, we suggest a context-aware correlation mitigation strategy that assists the CP engine to achieve the best accuracy regardless of the operating conditions. Learning from the previous results, in Table V, we summarize the recommended technique regarding each modality in each environment. When the vehicle enters a specific environment (e.g., based on the *a priori* knowledge of the map), the system could determine the most suitable technique and the associated attributes, before feeding them into the positioning engine to perform correlation mitigation. The aim is to match as close as possible to the accuracy of the optimal schemes under i.i.d measurements and accordingly, to provide a constant quality (i.e., highest accuracy) of the navigation service, while preserving low computational complexity.

TABLE V
INPUTS FOR CONTEXT-AWARE CORRELATION MITIGATION

Scenario	**Modality**	
	V2V RSSI	GPS position
Highway	adaptive sampling	differential measurement
Urban canyon	optional	differential measurement
Tunnel	differential measurement	N/A

VI. CONCLUSION AND FUTURE WORK

This paper contributes to the evaluation of CP in GPS-aided VANETs including realistic correlation effects. Simulation models for the GPS residual errors (i.e., 2-D error maps) and the shadowing process over V2V links (i.e., 4-D shadowing map) have been considered to capture the real-world spatial correlation of practical operating environments. On this occasion, we have first shown that this measurement noise correlation, if not handled carefully, is a threat to Bayesian filters/fusions. Then, two signal level and a protocol level approaches are proposed and can be combined to almost completely mitigate the deleterious correlation effects, including estimation of cross-link correlations (compensating for information loss), differential measurements (subtracting autocorrelations), and decreased fusion rate (collecting uncorrelated measurements) respectively. Sophisticated simulation experiments in canonical vehicular scenarios (urban canyon, tunnel, highway) show that the previous noise decorrelation techniques exhibit convincing performance gains over standard approaches that would neglect correlation. Apart from the specific tunnel environment, where decreasing the fusion rate does not seem appropriate, all the other cases lead to very high position accuracy. Beyond, the obtained results also highlight that there exists an optimal combination of correlation mitigation techniques depending on the operating environment and conditions, thus paving the way to context-aware solutions. Our evaluations take account of ad hoc communication and positioning manners, such as distributed and asynchronous position estimates or random CAM transmissions.

We have identified some directions for future work. Regarding positioning first, one aim is to benefit even further from correlation to go beyond the standard accuracy of i.i.d noise cases (e.g., by scheduling cooperative neighbors for uncorrelated data, by transmitting also raw unfiltered GPS data to extract correlation information...). Overall, we intend to refine our context-aware correlation mitigation strategies (e.g., by dynamically adjusting the assumed mobility model and implementing maneuvering car detection through innovation monitoring or multi-hypothesis filtering). New radio-based ranging (e.g., Ultra Wideband) and non-radio (e.g., inertial units) modalities shall be also integrated in the CP problem. As for communication aspects, the effects of congestion controls (i.e., power and/or rate controls) under ETSI DCC constraints, as well as message approximation, will be investigated in terms of particle-based CP accuracy, CAM overhead and resulting channel load. Finally, a dedicated traffic simulator [38] will be considered, generating realistic longer-term mobility traces that can mix several kinds of environments and regular/erratic mobility conditions. On this occasion, static and mobile NLoS effects shall be accounted too.

REFERENCES

[1] A. Boukerche, H. A. B. F. Oliveira, E. F. Nakamura, and A. A. Loureiro, “Vehicular ad hoc networks: A new challenge for localization-based systems,” *Computer Communications*, vol. 31, no. 12, pp. 2838–2849, 2008.

[2] C. R. Drane and C. Rizos, *Positioning Systems in Intelligent Transportation Systems*. Norwood, MA, USA: Artech House, Inc., 1st ed., 1998.

[3] D. Caveney, “Cooperative vehicular safety applications,” *IEEE Cont. Syst.*, vol. 30, pp. 38–53, Aug. 2010.

[4] “Intelligent Transport Systems (ITS); Vehicular Communications; Basic Set of Applications; Part 2: Specification of Cooperative Awareness Basic Service,” *ETSI Std. EN 302 637-2 V1.3.2*, Oct. 2014.

[5] “Vehicle Safety Communications-Applications (VSC-A), Final Report,” Tech. Rep. DOT HS 811 492A, U.S. Dept. Transp., Nat. Highway Traffic Safety Admin., Sept. 2011.

[6] G. M. Hoang, B. Denis, J. Härri, and D. T. M. Slock, “Distributed link selection and data fusion for cooperative positioning in GPS-aided IEEE 802.11p VANETs,” in *Proc. WPNC’15*, Mar. 2015.

[7] J. Yao, A. Balaei, M. Hassan, N. Alam, and A. Dempster, “Improving cooperative positioning for vehicular networks,” *IEEE Trans. on Veh. Technol.*, vol. 60, pp. 2810–2823, Jul. 2011.

[8] R. Parker and S. Valaee, “Vehicular node localization using received-signal-strength indicator,” *IEEE Trans. on Veh. Technol.*, vol. 56, pp. 3371–3380, Nov. 2007.

[9] N. Drawil and O. Basir, “Intervehicle-communication-assisted localization,” *IEEE Trans. on Intel. Transp. Syst.*, vol. 11, pp. 678–691, Sept. 2010.

[10] H. Noureddine Al Moussawi, *Some signal processing techniques for wireless cooperative localization and tracking*. Ph.D. dissertation, Télécom Bretagne, Université de Bretagne Occidentale, 2012.

[11] E. D. Kaplan and C. Hegarty, *Understanding GPS: Principles and Applications*. Boston, USA: Artech House, 2005.

[12] L. Mihaylova, D. Angelova, D. Bull, and N. Canagarajah, “Localization of mobile nodes in wireless networks with correlated in time measurement noise,” *IEEE Trans. on Mob. Comp.*, vol. 10, pp. 44–53, Jan. 2011.

[13] M. Gudmundson, "Correlation model for shadow fading in mobile radio systems," *Elect. Lett.*, vol. 27, pp. 2145–2146, Nov. 1991.

[14] N. Patwari and P. Agrawal, "Effects of correlated shadowing: Connectivity, localization, and RF tomography," in *Proc. ACM/IEEE IPSN'08*, pp. 82–93, Apr. 2008.

[15] D. Simon, *Optimal State Estimation: Kalman, H Infinity, and Nonlinear Approaches*. Newark, NJ, USA: Wiley, 2006.

[16] H. Li and F. Nashashibi, "Cooperative multi-vehicle localization using split covariance intersection filter," *IEEE Intel. Transp. Syst. Mag.*, vol. 5, pp. 33–44, Apr. 2013.

[17] Z. Wang, E. Tameh, and A. Nix, "Joint shadowing process in urban peer-to-peer radio channels," *IEEE Trans. on Veh. Technol.*, vol. 57, pp. 52–64, Jan. 2008.

[18] N. Patwari, A. Hero, M. Perkins, N. Correal, and R. O'Dea, "Relative location estimation in wireless sensor networks," *IEEE Trans. on Sig. Proc.*, vol. 51, pp. 2137–2148, Aug. 2003.

[19] H. Wymeersch, J. Lien, and M. Win, "Cooperative localization in wireless networks," *Proc. of the IEEE*, vol. 97, pp. 427–450, Feb. 2009.

[20] H. Lu, S. Zhang, X. Liu, and X. Lin, "Vehicle tracking using particle filter in Wi-Fi network," in *Proc. VTC'10-Fall*, Sept. 2010.

[21] L. Sun, Y. Wu, J. Xu, and Y. Xu, "An RSU-assisted localization method in non-GPS highway traffic with dead reckoning and V2R communications," in *Proc. CECNet'12*, pp. 149–152, Apr. 2012.

[22] N. Patwari, J. Ash, S. Kyperountas, A. Hero, R. Moses, and N. Correal, "Locating the nodes: Cooperative localization in wireless sensor networks," *IEEE Sig. Proc. Mag.*, vol. 22, pp. 54–69, Jul. 2005.

[23] T. Abbas, K. Sjöberg, J. Karedal, and F. Tufvesson, "A measurement based shadow fading model for vehicle-to-vehicle network simulations," *Int. J. of Ant. and Prop.*, vol. 2015, 2015.

[24] F. Gustafsson, F. Gunnarsson, N. Bergman, U. Forssell, J. Jansson, R. Karlsson, and P.-J. Nordlund, "Particle filters for positioning, navigation, and tracking," *IEEE Trans. on Sig. Proc.*, vol. 50, pp. 425–437, Feb. 2002.

[25] F. Bai and A. Helmy, *A survey of mobility models in wireless ad hoc networks*. University of Southern California, 2006.

[26] "Minimum operational performance standards for Global Positioning System/Wide area augmentation system airborne equipment," Tech. Rep. DO-229D, RTCA, Inc., 2006.

[27] X. Cai and G. Giannakis, "A two-dimensional channel simulation model for shadowing processes," *IEEE Trans. on Veh. Technol.*, vol. 52, pp. 1558–1567, Nov. 2003.

[28] Z. Sahinoglu, S. Gezici, and I. Gvenc, *Ultra-wideband Positioning Systems: Theoretical Limits, Ranging Algorithms, and Protocols*. New York, NY, USA: Cambridge University Press, 2011.

[29] G. Acosta-Marum and M. A. Ingram, "Six time- and frequency- selective empirical channel models for vehicular wireless LANs," *IEEE Veh. Technol. Mag.*, vol. 2, pp. 4–11, Dec. 2007.

[30] H. Tchouankem, T. Zinchenko, and H. Schumacher, "Impact of buildings on vehicle-to-vehicle communication at urban intersections," in *Proc. CCNC'15*, pp. 206–212, Jan. 2015.

[31] M. Boban, T. T. V. Vinhoza, M. Ferreira, J. Barros, and O. K. Tonguz, "Impact of vehicles as obstacles in vehicular ad hoc networks," *IEEE JSAC*, vol. 29, pp. 15–28, Jan. 2011.

[32] M. Boban, J. Barros, and O. Tonguz, "Geometry-based vehicle-to-vehicle channel modeling for large-scale simulation," *IEEE Trans. on Veh. Technol.*, vol. 63, pp. 4146–4164, Nov. 2014.

[33] G. M. Hoang, B. Denis, J. Härri, and D. T. M. Slock, "Select thy neighbors: Low complexity link selection for high precision cooperative vehicular localization," in *Proc. VNC'15*, Dec. 2015.

[34] M. Arulampalam, S. Maskell, N. Gordon, and T. Clapp, "A tutorial on particle filters for online nonlinear/non-Gaussian Bayesian tracking," *IEEE Trans. on Sig. Proc.*, vol. 50, pp. 174–188, Feb. 2002.

[35] G. M. Hoang, B. Denis, J. Härri, and D. T. M. Slock, "On communication aspects of particle-based cooperative positioning in GPS-aided VANETs," in *Proc. CCP IV'16*, Jun. 2016.

[36] J. Kunisch and J. Pamp, "Wideband car-to-car radio channel measurements and model at 5.9 GHz," in *Proc. VTC'08-Fall*, Sept. 2008.

[37] L. Cheng, B. E. Henty, F. Bai, and D. D. Stancil, "Highway and rural propagation channel modeling for vehicle-to-vehicle communications at 5.9 GHz," in *Proc. AP-S'08*, pp. 1–4, Jul. 2008.

[38] D. Krajzewicz, G. Hertkorn, C. Rssel, and P. Wagner, "SUMO (Simulation of Urban MObility) - An open-source traffic simulation," in *Proc. MESM'02*, pp. 183–187, Sept. 2002.

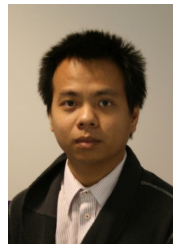

Gia-Minh Hoang received his M.Sc. degree in electronics and telecommunications from the University of Rennes 1 (Rennes, France) in 2014. He worked on location-enabled wireless body area networks as research assistant with the French Institute for Research in Computer Science and Automation (INRIA) and the French Institute for Research in IT and Random Systems (IRISA) in 2013–2014. He has been currently pursing a Ph.D. degree in electronics and communications from Télécom ParisTech (Paris, France), jointly prepared at the French Commission for Alternative and Atomic Energies (CEA) (Grenoble, France) and EURECOM (Sophia Antipolis, France). His current research interests cover various aspects of mobile communications and localization for Intelligent Transport Systems (ITS).

Benoît Denis received the E.E. (2002), M.Sc. (2002), and Ph.D. (2005) degrees from INSA (Rennes, France) in electronics and communication systems. Since December 2005, he has been with CEA-Leti Minatec (Grenoble, France), contributing into French (ANR), European (FP6/FP7/H2020) and extra-European (QMIC) collaborative research projects in the fields of wireless sensor and wearable networks, heterogeneous and cooperative networks, vehicular networks, mobile applications related to the Internet of Things and Intelligent Transportation Systems (e.g. PULSERS II, eUWB, eSENSE, SENSEI, WHERE 1 & 2, BUTLER, SocIoTal, CORMORAN, CROW^2, HIGHTS...). His research interests include radio technologies for joint wireless localization and communications, ranging/positioning/tracking and hybrid data fusion algorithms, radio channel modeling and PHY/MAC cross-layer protocol design.

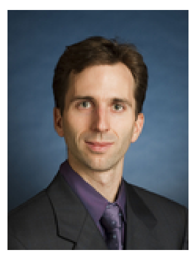

Jérôme Härri is Assistant Professor at the Mobile Communication Group at EURECOM, France, and conducting research in wireless vehicular networks. Previously, he led the Traffic Telematics Junior Research Group at the Institute of Telematics of the Karlsruhe Institute of Technology (KIT), Germany. His research interests are related to the optimization of the vehicular wireless channel usage, to the investigation of cooperative ITS strategies and to the characterization of the mutual relationship between vehicular mobility and heterogeneous vehicular communication. He has authored and co-authored over 60 international journal and conference papers, and is involved in various National and European research projects related to wireless vehicular communications. He holds a M.Sc. degree and a Dr. s sc. degree in telecommunication from the Swiss Institute of Technology (EPFL), Lausanne, Switzerland.

Dirk T.M. Slock received an engineering degree from the University of Ghent, Belgium, in 1982, and the M.S. degree in electrical engineering (1986), M.S. degree in statistics (1989), and Ph.D. degree in electrical engineering (1989), all from Stanford University (Fulbright grant). He has been a professor at EURECOM since 1991. He invented semiblind channel estimation, the chip equalizer-correlator receiver (3G), MIMO-CDD now part of LTE, and the Single Antenna Interference Cancellation (SAIC) (GSM standard). He has (co)authored 420 papers. He received a Best Paper Award from the IEEE Signal Processing Society and from EURASIP in 1992, and two IEEE Globecom98, one IEEE SIU04 and one IEEE SPAWC05 Best Student Paper Award.